The title of your thesis

Sholto O. Forbes-Spyratos

B.Eng. (Mechanical and Aerospace) (Hons. I) & B.Sc. (Physics) UQ

Abstract

Declaration by author

This thesis is composed of my original work, and contains no material previously published or written by another person except where due reference has been made in the text. I have clearly stated the contribution by others to jointly-authored works that I have included in my thesis.

I have clearly stated the contribution of others to my thesis as a whole, including statistical assistance, survey design, data analysis, significant technical procedures, professional editorial advice, and any other original research work used or reported in my thesis. The content of my thesis is the result of work I have carried out since the commencement of my research higher degree candidature and does not include a substantial part of work that has been submitted to qualify for the award of any other degree or diploma in any university or other tertiary institution. I have clearly stated which parts of my thesis, if any, have been submitted to qualify for another award.

I acknowledge that an electronic copy of my thesis must be lodged with the University Library and, subject to the policy and procedures of The University of Queensland, the thesis be made available for research and study in accordance with the Copyright Act 1968 unless a period of embargo has been approved by the Dean of the Graduate School.

I acknowledge that copyright of all material contained in my thesis resides with the copyright holder(s) of that material. Where appropriate I have obtained copyright permission from the copyright holder to reproduce material in this thesis.

Publications during candidature

Journal papers

Denman2016a

Denman2016b

Conference papers

Denman2014

Denman2016c

Technical reports

Denman2017

Publications included in this thesis

This thesis comprises partly of publications, as allowed by University of Queensland Policy PPL 4.60.07. The papers that have been included have all been published in peer reviewed journals at the time of submission.

Denman2016a

Contributor	Contribution
Zachary J. Denman	Experimental design (90%)
	Performed simulations (60%)
	Performed experiments (95%)
	Analysis of results (85%)
	Wrote and edited paper (80%)
Wilson Y. K. Chan	Performed experiments (5%)
	Analysis of results (10%)
	Wrote and edited paper (2.5%)
Stefan Brieschenk	Experimental design (2.5%)
Ananthanarayanan Veeraragavan	Experimental design (2.5%)
	Analysis of results (10%)
	Wrote and edited paper (10%)
Vincent Wheatley	Experimental design (2.5%)
	Performed simulations (40%)
	Analysis of results (10%)
	Wrote and edited paper (5%)
Michael K. Smart	Experimental design (2.5%)
	Analysis of results (5%)
	Wrote and edited paper (2.5%)

Denman2016b

Contributor	Contribution
Zachary J. Denman	Experimental design (100%) Analysis of results (85%) Wrote and edited paper (80%)
Ananthanarayanan Veeraragavan	Experimental design (2.5%) Wrote and edited paper (10%)
Vincent Wheatley	Experimental design (2.5%) Wrote and edited paper (5%)
Michael K. Smart	Experimental design (2.5%) Analysis of results (5%) Wrote and edited paper (2.5%)

Contributions by Others to the Thesis

Except for the contributions by others to publications above, there are no contributions by others to this thesis.

Statement of Parts of the Thesis Submitted to Qualify for the Award of Another Degree

None.

Acknowledgements

Write your acknowledgements here. Put a funny quote at the bottom. This is the one I used.

In theory, there is no difference between theory and practice. But, in practice, there is.

— Jan L.A. van de Snepscheut

Keywords

keyword, keyword, keyword, keyword, keyword

Australian and New Zealand Standard Research Classification (ANZSRC)

ANZSRC code: 090107 Hypersonic Propulsion and Hypersonic Aerodynamics, 100%

Fields of Research (FoR) Classification

FoR code: 0901, Aerospace Engineering, 100%

CONTENTS

LIST OF FIGURES

LIST OF TABLES

CHAPTER 1

INTRODUCTION

This is where your introduction goes. There will probably be a some references here (**Denman2016a**). The previous citation was done using the `parencite` command. There is also which the `textcite` command for in text citations. For instance, **Colket2001** is a product of the `textcite` command. Figure 1.1 shows you what a figure is. Remember to update the `graphicspath` in the `packages.tex` file as you write your thesis.

This template uses the `nomencl` package. Have a look at the lines below this paragraph in the `1_introduction.tex` file to see how this works. Also take a look at lines 21–49 in `packages.tex` to see the groupings available.

The remainder of your introduction should include your thesis aim and objectives and a chapter summary.

1.1 Research aims

The overall aim of this thesis is to

make scramjets fly.

This will be achieved through the following objectives:

1. *Flying them*
   Flying scramjets will conclusively prove that scramjets can fly.

2. *Fly different types of scramjets*
   By flying lots of scramjets we can see that they are awesome.
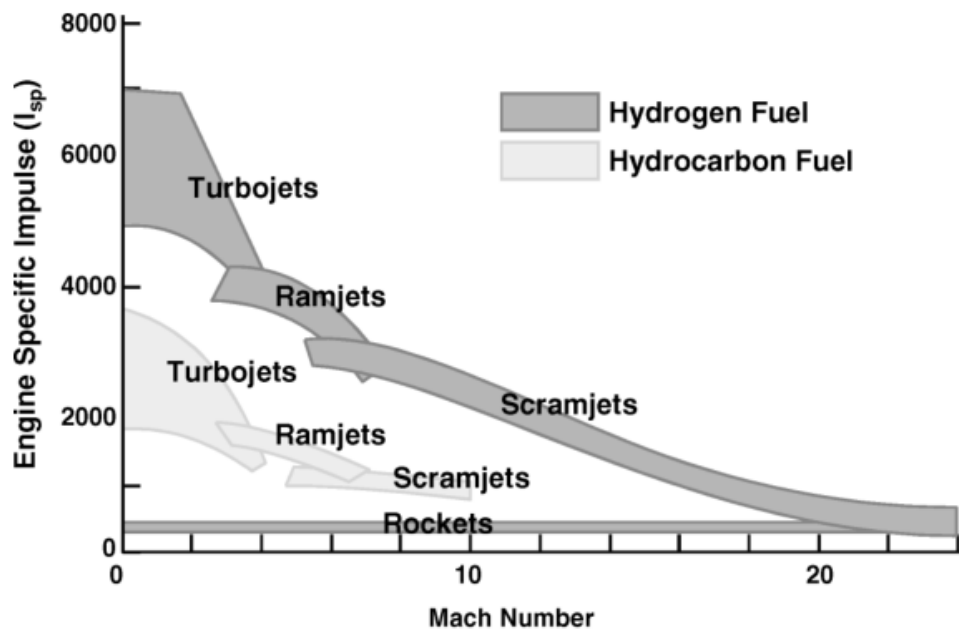
Figure 1.1: Specific impulse of various engine types for hydrogen and hydrocarbon fuels (**Fry2004**)

3. *Having 3 objectives is typically good.*
   Three objectives just makes this section look complete.

1.2 Thesis outline

Edit this as required. This thesis is organised in eight chapters which are outlined below. The appendices included at the end of this document contain further technical information and supplementary experimental details. If you want to add colours to the text for some reason (supervisor reviewing etc.), use the `textcolor` command. Check the code here to see how.

Chapter 2 - Literature review

This chapter presents a review of literature related to the different aspects of this thesis.

Chapter 3 - Methodology

This chapter provides details of the experimental facility, experimental model, and test conditions used in the completion of the experiments that form the majority of this thesis.

Conclusions

The body of this thesis concludes by summarising the most significant findings from Chapters **??** through 6. Recommendations for future studies on cavity flameholders in three-dimensional, hydrocarbon-fuelled scramjet engines, such as the REST engine, are provided.

CHAPTER 2

LITERATURE REVIEW

This chapter examines the relevant literature associated with the different aspects of the work conducted as part of this thesis. Explain order and of literature and what was examined.

2.1 Airbreathing Access to Space Systems

The possibility of using airbreathing stages in access to space systems has been studied in some detail, and there are multiple systems currently under preliminary development. These systems have been investigated in various forms including; single stage, dual stage and tri stage designs. Single stage designs are currently undergoing evaluation, the most prominent of which is the SKYLON Spaceplane being developed by Reaction Engines Limited **Varvill2004**. The SKYLON is a spaceplane which utilises SABRE, a combined cycle airbreathing rocket propulsion system potentially reusable for 200 flights, and is being developed to deliver payloads on the order of 2800kg to heliosynchronous orbit **Sky-rel-ma-**.

A single stage design has the advantage of being fully contained within one vehicle, which is convenient for reusability and return trajectories however is has been suggested by Smart & Tetlow **Smart2009** that these designs suffer from severe limitations as they must contain multiple engines which add mass at later stages of the trajectory and decrease the efficiency of the vehicle. Smart & Tetlow suggest that multistage systems offer significant improvements in payload mass fractions, and have the advantage of using airbreathing stages only within their operable range. Dual stage designs have been investigated in some detail using the 'spaceplane' concept by Mehta & Bowles **Mehta2001** using life cycle cost analysis in order to take flexibility and reusability into account. Mehta & Bowles conclude that a two stage design is the optimal configuration for reusable hypersonic space access systems, however this study is only based on comparison with single stage to orbit systems, and it

5

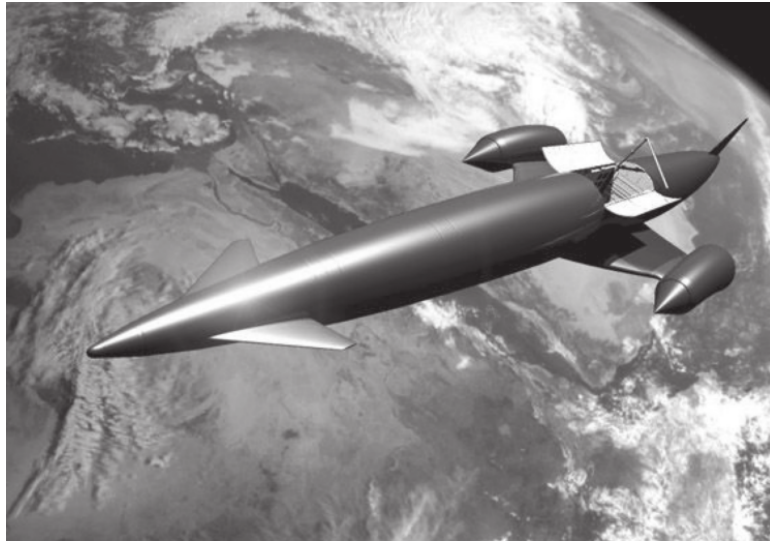
Figure 2.1: The SKYLON spaceplane **Varvill2008**.

is more useful to consider their conclusions as an endorsement of multi stage airbreathing designs in general. They find that multi stage vehicles have higher potential for payload that single stage to orbit (SSTO) systems and have less propellant requirements, partly due to a greater atmospheric cruise capability.

2.2 Scramjets

A Scramjet, or supersonic combustion ramjet, is an airbreathing engine design which combusts air at supersonic speeds and is capable of high Mach number operation. Scramjets were proposed in the 1940's **Curran2001** and found to be capable of positive net thrust in 1993 **Paull1993** but have yet to be developed to a level which would allow for commercial application. Scramjet powered vehicles are a primary candidate for small payload delivery systems, offering much higher specific impulse than rockets over their operating range **Billig1993 Cook2003**. Scramjet engines exhibit this advantage within their operating range of Mach 6-12 due to using atmospheric oxygen for reaction and only carrying fuel, increasing the payload mass that the scramjet vehicle is able to carry. Figure 2.2 shows the operating corridor for scramjet engines, indicating the point at which transition to rocket stage would occur, the lower dynamic pressure limit on engine operation and the upper dynamic pressure limit on the aircraft structure.

Smart & Tetlow **Smart2009** have found that the fuel savings achieved by using a scramjet engine within these limits, coupled with small necessary payload mass, may enable the development of a partially or fully reusable space access system utilising a scramjet powered stage in the near future. Simulations carried out for three stage systems utilising scramjet and rocket engines for small payload delivery show possible payload mass fractions of around 1.5% to 200km orbit with a reusable scram-
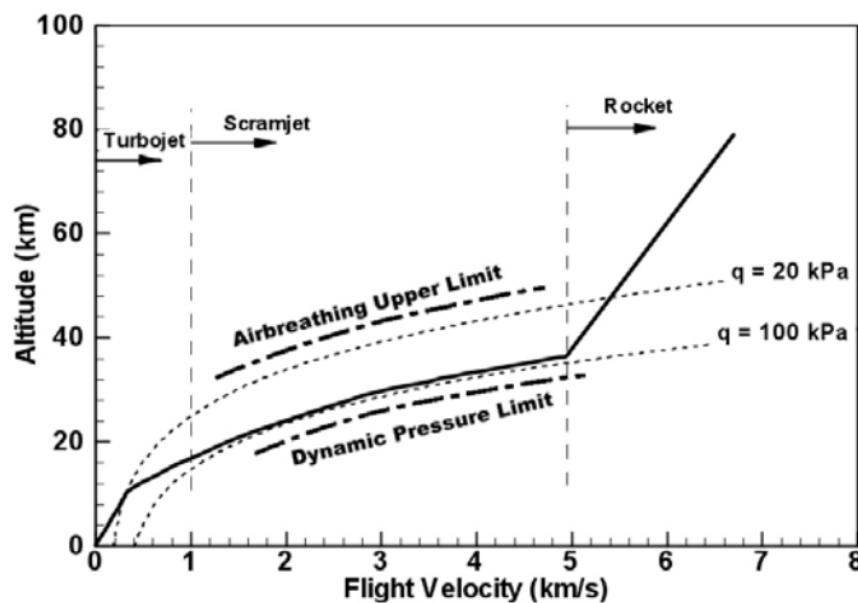
Figure 2.2: The airbreathing vehicle flight corridor **Smart2010**.

jet stage **Smart2009**. Scramjet powered vehicles may also offer the ability to put small payloads into orbit with greatly increased flexibility and launch window when compared to similarly sized rocket systems. This has been assessed in a study by Flaherty **Flaherty2010** comparing the United States Air Force's Reusable Military Launch System all-rocket launch vehicle RMLS102 against the Alliant Techsystems rocket/scramjet launch system ATK-RBCC. These vehicles are similarly sized and comparisons were made for payloads launched to rendezvous with satellites in randomly generated orbits. These vehicles were compared using the range of orbital trajectories that each vehicle was able to rendezvous with within one day, determined by launch vehicle range. The rocket/scramjet ATK-RBCC was found to have a large advantage in trajectory flexibility over the rocket only vehicle, in a large part due to the scramjets ability to fly fuel efficiently over long distances. This means in general that a partially scramjet powered accelerator is able to fulfil the specific delivery needs of small payloads over a wider range of orbits within smaller time periods when compared to a fully rocket powered accelerator. This can be advantageous for time critical and orbit dependant payloads which have specific mission requirements to be met.

2.3 The SPARTAN

The University of Queensland is developing a three stage partially reusable access to space system utilising the SPARTAN scramjet powered vehicle as the reusable second stage shown in Figure 2.3 **Jazra2013**. This is the system which is considered in this study and is used as a representative system for three stage airbreathing access to space system designs. This system is designed for small

payload deliveries to orbit and will utilise the ALV rocket booster to accelerate the SPARTAN stage to minimum Mach number required for stable burn, at which point separation occurs and the second stage uses a scramjet engine to accelerate to between Mach 6-10.
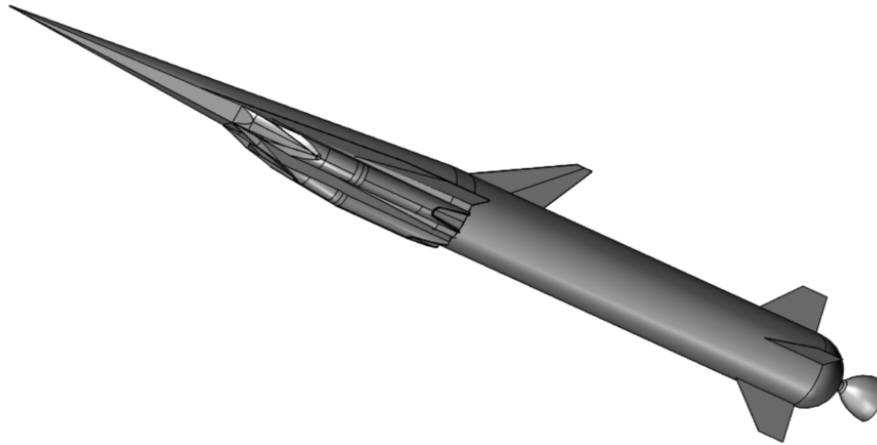

Figure 2.3: The SPARTAN system **Jazra2013**.

The third stage will be a disposable rocket stage, which will then deliver the payload to orbit via a pull up manoeuvre to leave the atmosphere, followed by a Hohmann transfer. The first and second stages will be reusable, the first stage via conversion into a propeller powered drone, and the second stage through either a glide or extra scramjet powered flight to a suitable landing site.

This system has been designed to initial design stages, with estimates of payload mass fraction indicating that 1.26% PMF is possible when delivering a 257.4kg payload to low earth orbit **Preller2015a**. This compares well with existing space systems of similar size, with the advantage of being designed for reusability. The second stage vehicle has been designed to a detailed level, and optimised for payload delivery to heliosynchronous orbit. The first stage ALV is being designed by Heliaq engineering and is in initial testing stages.

The SPARTAN has been studied in some detail, simulating over a constant dynamic pressure trajectory and varying the aerodynamic surface properties of the vehicle.

2.3.1 Scramjet Engine Model

To deliver a payload to orbit, the SPARTAN uses four Rectangular-to-Elliptical Shape Transition (REST) scramjet engines, with inlets configured to allow installation on a conical forebody. This study uses engines configured to fly between Mach 5 and 10, this type of engine is known as a C-RESTM10 engine**Preller2017**. The REST model has been studied experimentally for flight at off design conditions by Smart & Ruf **Smart2006**. The REST engine has been used as it has been proven to operate successfully at off-design conditions, an extremely important property for this study as the scramjet stage experiences a range of Mach number flight conditions, and significant variation in
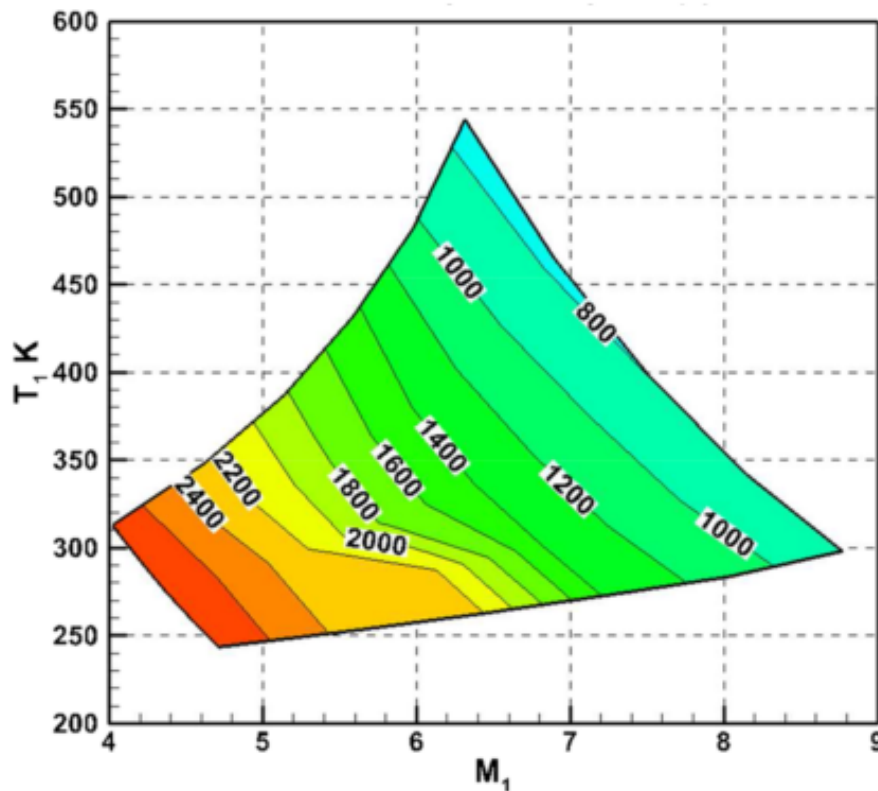
Figure 2.4: The C-RESTM10 propulsion database, specific impulse.

dynamic pressure.

A propulsion database of the C-RESTM10 has been provided for this study by Prof. Michael Smart.

2.4 First Stage Rocket Boosters

The SPARTAN scramjet vehicle must be accelerated to its minimum operating speed by a first stage rocket booster. This booster must be capable of efficient operation from launch at sea level until staging. It is envisioned that the SPARTAN system will eventually use a reusable flyback booster**Preller2017**. However the flyback of the first stage is outside the scope of this study. Instead, a model of an existing first stage booster will be used, for which the Falcon-1e was chosen.

The SPARTAN mission requires a relatively small, modern booster.

-why did we choose the Falcon -compare to other, similar engines HM-60 and LE-7 are closest (they are still double the thrust.. so maybe cant compare these too well)

The SpaceX Falcon-1e launch system was a proposed small satellite launch system which would have entered use after 2010**Vehicle2008**, but was discontinued and superseded by the Falcon-9 project. The Falcon-1e was designed to launch payloads between 600-900kg to low Earth orbit, with flex-

ible orbit altitude and inclination. The first stage of the Falcon-1e is powered by a Merlin 1C LOX/Kerosene turbopump engine.

2.5   Exoatmospheric Rocket Engines

After scramjet stage burnout, the upper stage rocket must exit the atmosphere, and accelerate the payload to orbital velocity. This requires a rocket engine with sufficient thrust to accelerate the third stage rocket out of the atmosphere, and a diameter small enough to allow the rocket to fit within the fuselage of the SPARTAN. Table 2.1 shows a comparison study of upper stage rocket engines.

Engine	Fuel Supply	Fuel	Thrust	Isp	Mass	Diameter	Length	Thrust Vector Capability
Aestus	Pressure-fed	MMH/NTO	27.5kN	320s	110kg	1.27m	2.2m	4° & 4° by mechanical adjustment
OMS	Pressure-fed	MMH/NTO	26.7kN	316s	118kg	1.168m	1.956m	8°
Aestus II	Pump-fed	MMH/NTO	46kN	337.5s	148		2.2m	
RS-72	Pump-fed	MMH/NTO	55.4kN	338s	154kg		2.286	
ATE	Pump-fed	MMH/NTO	20kN	345s	57.9kg	0.38m	1.4m	
AJ10-118K	Pressure-fed	A-50/NTO	43.3kN	320.5s	124.5kg	1.53m	2.7m	
Kestrel								
Rl-10-3A								

Table 2.1: Comparison of upper stage rocket engines.

2.6   Partially-Airbreathing Launch Vehicle Ascent Trajectories

Current simulations of the SPARTAN vehicle have been carried out with the assumption of a 50kpa dynamic pressure trajectory, a likely design point of the vehicle and scramjet engine. Constant dynamic pressure trajectories have been used for airbreathing vehicle simulation due to the tradeoff between structural loading and engine performance for hypersonic vehicles **Olds1998** . As dynamic pressure increases so does the structural loading on the vehicle, however scramjet thrust is directly reliant on dynamic pressure ie. an increase in dynamic pressure directly means more air into the engine inlet. A constant dynamic pressure is viewed as being an acceptable compromise between these two factors. This form of trajectory has so far been simulated using proportional integral derivative (PID) feedback control, directly investigated since 1998 by Olds & Budianto **Olds1998**. This is a simple and effective form of control for systems being simulated over a constant dynamic pressure path **Preller2015**. This form of control utilises minimises an error function as the vehicle moves along its trajectory. This error function causes the controls of the vehicle to be modified by a feedback term which is a function of the error including proportional, integral and derivative terms. The result is a trajectory which is suitably close to the objective design point, with minimal overshoot and steady state error which can cause oscillations around the specified design value. Figure 2.5 shows an example of a constant gain PID controller as applied to the SPARTAN vehicle being simulated to a design point of 50kPa dynamic pressure. Oscillations can be observed around the design point due to overshoot and steady state error, factors which are prevalent in PID control systems.
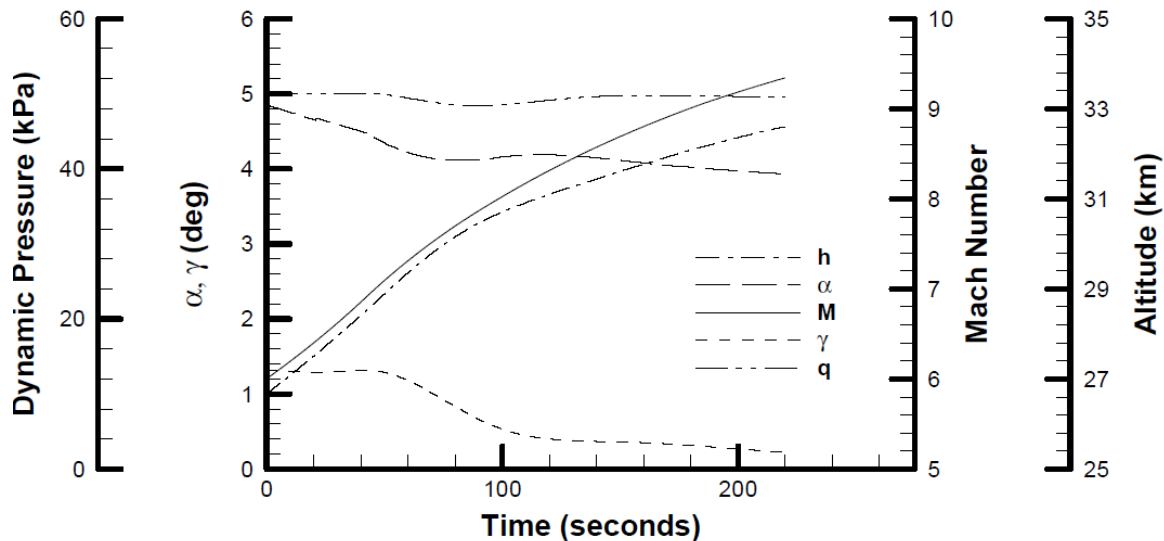

Figure 2.5: An example of a constant gain PID controller, controlling the SPARTAN trajectory around a 50kPa dynamic pressure design point **Preller2015**.

It is possible that a constant dynamic pressure trajectory may not be the most appropriate trajectory for the second stage vehicle, as there is a variety of aerodynamic factors that must be considered

in designing optimal payload to orbit flight. It may be optimal for the vehicle to fly at less than maximum dynamic pressure at point throughout the trajectory, most likely at the first to second and second to third stage separation points. For a constant dynamic pressure trajectory the second-third stage transition will occur at a very low trajectory angle. This is suboptimal for the third stage rocket, which needs to perform a large pull up manoeuvre at high dynamic pressure. Launching this system at higher angle or altitude may improve third stage fuel usage greatly, at a small cost to the second stage fuel, allowing a greater payload to be delivered to orbit.

2.6.1 Single-Stage Vehicles

Optimal trajectories have previously been developed for launch systems integrating airbreathing and rocket propulsion within single-stage-to-orbit (SSTO) vehicles **Powell1991**; **Lu1993**; **Trefny1999**. These optimal trajectory studies found unanimously that a pull-up manoeuvre before the end of the airbreathing engine cut-off was the optimal flight path for the SSTO airbreathing-rocket vehicles being investigated. A pull-up was found to be optimal for vehicles where the rocket engines are not ignited until circularization altitude **Powell1991**; **Lu1993** as well as vehicles where the rocket engine is ignited immediately after airbreathing engine cut-off **Trefny1999**. For SSTO vehicles a pull-up manoeuvre is a simple trade-off between the altitude at airbreathing engine cut-off and the velocity achievable at cut-off. Due to the entire vehicle being lifted into orbit, this becomes a relatively simple problem of engine efficiency. The airbreathing engine is used for its high efficiency, until the dynamic pressure drops below the operable limit of the airbreathing engine, or until the thrust provided by the airbreathing engine is significantly counteracted by the effects of drag and gravity.
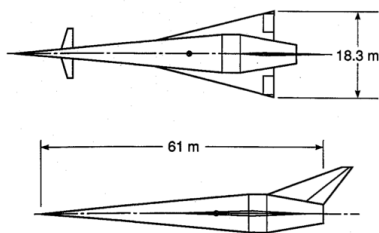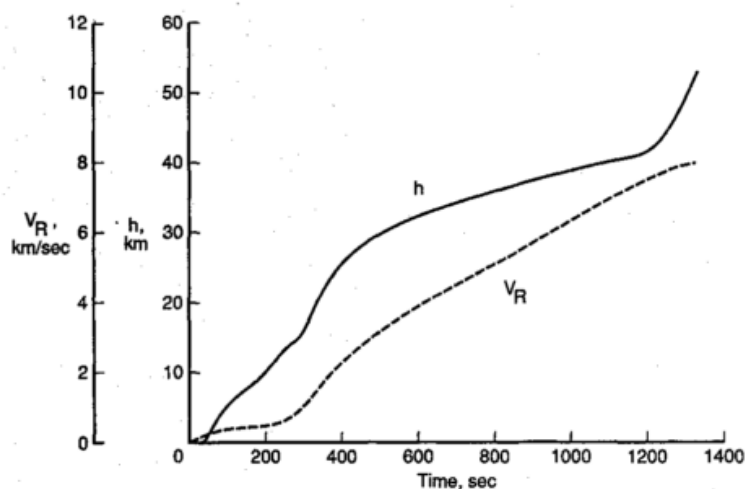

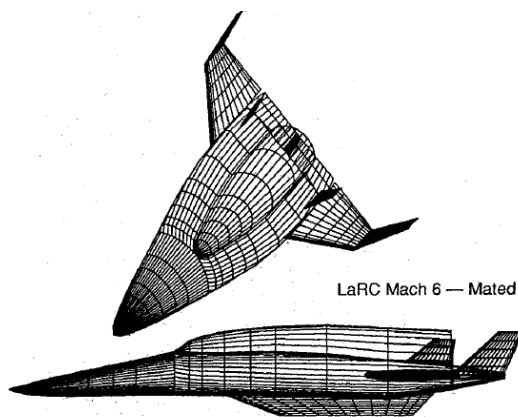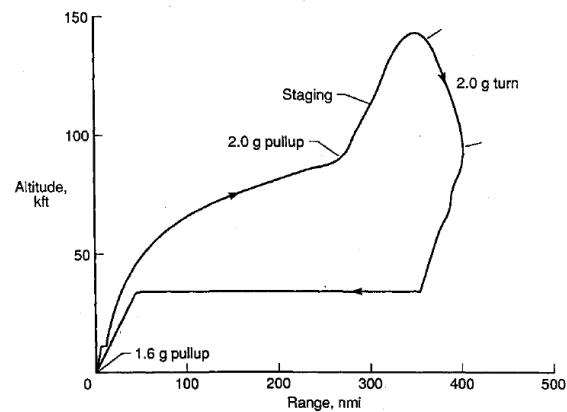Figure 2.6   Figure 2.7: Powell

Figure 2.8

Figure 2.9: Wilhite

2.6.2 Multi-Stage Vehicles

For a multi-stage to orbit vehicle, calculating the optimal trajectory for maximum payload flight is significantly more difficult. A multi-stage vehicle has one or more stage transition points, where the vehicle separates a component which is discarded or reused later, and does not continue to orbit. At a stage transition point there is a large change in the mass and aerodynamics of the launch system. This change in flight dynamics makes finding the optimal stage transition point more complicated. To find the optimal separation point there is a trade-off between: I. The high efficiency of the scramjet engines, II. The thrust produced by the scramjet engines, III. The potential thrust of the rocket engines, IV. The energy necessary to increase the altitude of the scramjet stage, V. The aerodynamic efficiency when performing the required direction change. All of these factors must be considered in order to generate an optimal trajectory.

There has been a number of studies which have identified a pull-up manoeuvre as being advantageous for a multi-stage system **Tsuchiya2005**; **Wilhite1991**; **Mehta2001**. However, in these studies a pull-up manoeuvre has been specified in order to decrease the dynamic pressure of the vehicle at airbreathing-rocket stage separation.

-talk about the vehicles being analysed (mention TSTO)

In the studies by Tsuchiya et al.**Tsuchiya2005** and Wilhite et al.**Wilhite1991**, decreased dynamic pressure is necessary for the successful operation of the orbital rocket stages, of the systems under investigation. In these studies the airbreathing stages pull-up to the maximum allowable dynamic pressure for the rocket-powered orbital stages. When the orbital stages are able to operate, stage separation occurs. These pull-up manoeuvres demonstrate the advantages of a pull-up for the operation of the orbital stages, allowing the aerodynamic and thermal loading on the vehicle to be reduced. However these pull-up manoeuvres are not performed as part of optimal trajectories, instead they are designed to ensure that the performance constraints of the systems are met.

Mehta & Bowles **Mehta2001** prescribe a 2g pull-up at flight conditions of Mach 10, 95000 ft
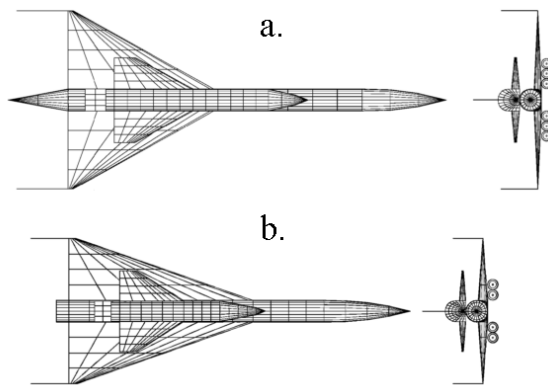
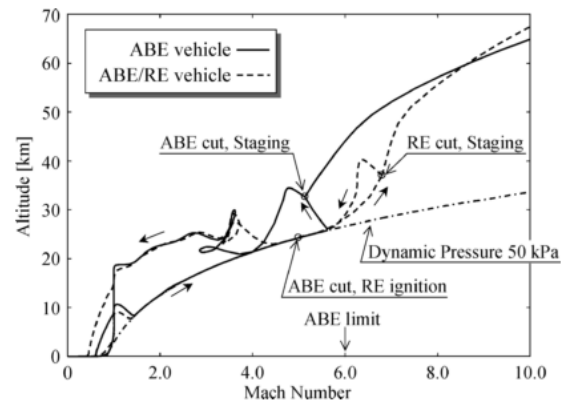Figure 2.10: a) Airbreathing b) Airbreathing/Rocket
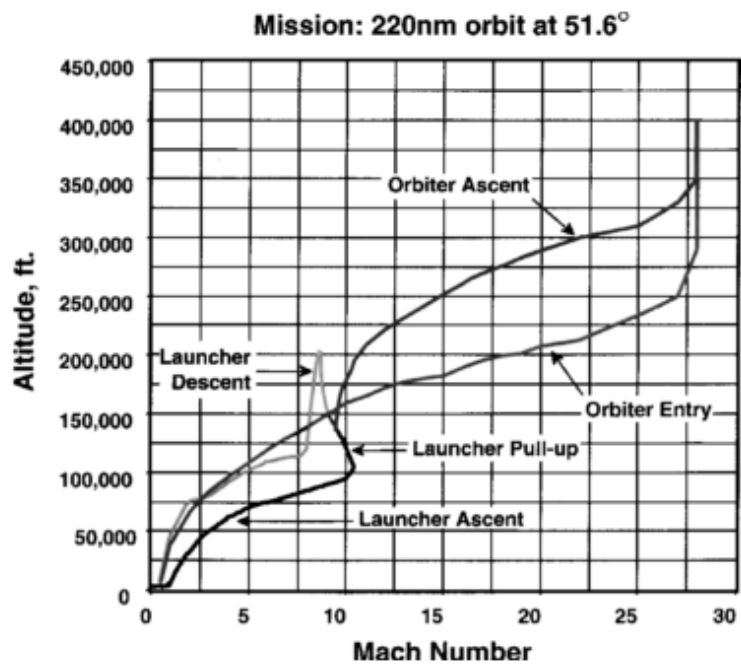

Figure 2.11: Tsuchiya

Figure 2.12

Figure 2.13: Mehta

for an airbreathing stage in order to "lower dynamic pressures and to achieve the optimal launching flight path angle for the orbiter vehicle". This indicates that a pull-up manoeuvre before airbreathing-rocket transition is considered the optimal trajectory, however this study does not optimise the shape or magnitude of the pull-up manoeuvre, only considering the increased performance of the rocket vehicle.

2.7 Hypersonic Vehicle Flyback Trajectories

THIS SECTION IS VERY ROUGH!

full flyback is important to us, but i should look at some partial flyback cases too (look at federicos paper)

mention skipping vs constant descent at max L/D (need to look at why this is)

Due to the second-third stage staging velocity, the SPARTAN may be incapable of turning fast enough to cover the necessary fly-back distance. Multiple studies have investigated the maximum staging velocity allowable for the glide-back flight of a booster. Tetlow et al. CITATION compare powered cruise-back to glide-back flight for the return of the first stage booster of a rocket powered two-stage launch vehicle. The powered flyback vehicle uses airbreathing engines to cruise back to the launch site at relatively low speeds. The powered flyback and the glide-back cases are analysed separately to determine the difference in the optimal staging velocities. Figure 2 shows the optimised deceleration phase for the cruise-back vehicle, terminating at cruise-back conditions. This trajectory shows three distinct skips, with the minimum trajectory angle progressively decreasing between each. The powered cruise-back vehicle is able to stage at 3000m/s due to the ability to cover a large distance during cruise-back. The glide-back vehicle was optimised to find the maximum possible staging velocity at which a turn and glide-back is still possible. This was found to be at 1200m/. Figure 3 shows the corresponding optimal deceleration trajectory, terminating at sustainable glide conditions. This trajectory again shows multiple skips. The low allowable separation velocity of 1200m/s for the glide-back booster potentially suggests that the SPARTAN will require powered flyback. Tetlow et al. assume an admittedly optimistic L/D of 7 at Mach 0.9, and maximum angle of attack of 40 deg. However, the mass of the vehicle in this study is up to 1182 tons. A lower L/D may be acceptable for a lighter vehicle.

A maximum staging velocity at which glide-back is possible is also investigated by Hellman CITATION. Hellman uses a suboptimal, scheduled trajectory simulation to investigate the flyback capabilities of a reusable rocket booster. Hellman finds that Mach 3 is the upper staging limit for a glide-back booster. This agrees with Tetlow et al. that high staging velocities are not possible for glide-back boosters, suggesting that the SPARTAN will require powered return flight.

The possibility of an airbreathing vehicle reigniting high speed airbreathing engines for short periods has been investigated by Tsuchiya and Mori **Tsuchiya2005**. Tsuchiya and Mori investigate a
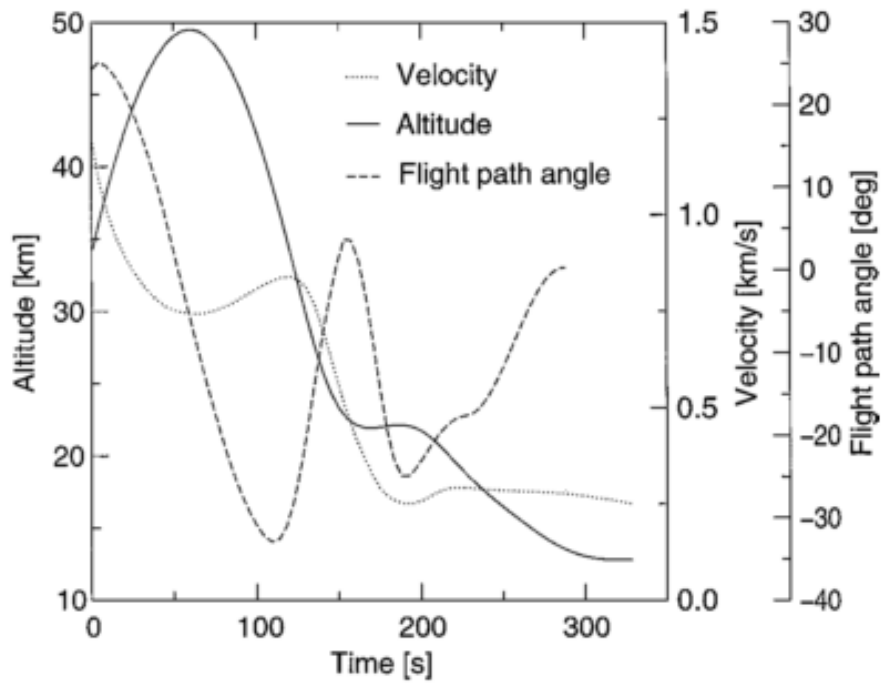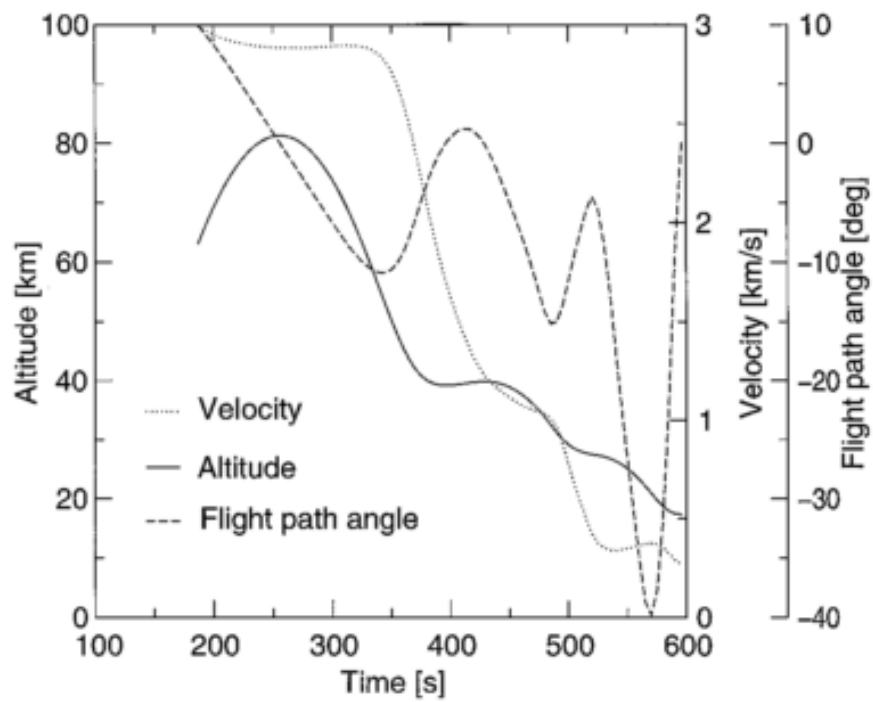
Figure 2.14

Figure 2.15

two-stage-to-orbit spaceplane, comparing two first stage configurations; an airbreathing accelerator and an accelerator with combined airbreathing/rocket propulsion. For the purposes of flyback there vehicles are very similar, both using the high speed airbreathing engines during return flight. The optimal launch trajectories for these vehicles is shown in Figure **??**. The separation for the airbreathing vehicle occurs at Mach 5.1, and the separation for the airbreathing/rocket vehicle at Mach 6.8. Both optimised return trajectories follow a relatively similar path. A long skip is performed, with both vehicles hitting the dynamic pressure limit. Both vehicles ignite the airbreathing engines at around Mach 3.5 for several tens of seconds to extend the range of the flyback manoeuvres. After this, the vehicles descend and land at the launch site. The velocity at the landing point is not constrained, causing the airbreathing vehicle to land at slightly under Mach 1, and the airbreathing-rocket vehicle to land at approximately Mach 0.5. The latter is comparable with the landing velocity of the space shuttle **Romere1983**.

The SPARTAN is designed to separate the third stage above Mach 9. This is considerably higher than the separation velocities of the vehicles in the study by Tsuchiya and Mori. The SPARTAN will also release into a dynamic pressure considerably higher than 15kPa, and it is desired to land the SPARTAN at a comparably low velocity.

2.8   Optimal Control

To this point analysis of the SPARTAN trajectory has been performed using PID feedback control, assuming a constant dynamic pressure trajectory **Preller2015**. PID feedback control simulates the vehicle flight and manoeuvres the vehicle so that the trajectory conforms to a defined design point. Currently the trajectory of the SPARTAN has been simulated to align as closely as possible with 50kPa flight, a problem for which PID control is well suited.

This study aims to find the optimal trajectory path for the SPARTAN that will produce maximum payload to orbit capability for the three stage system. Feedback control is infeasible for finding an optimal trajectory shape as there is no single design point at each stage of the simulated trajectory to calibrate towards. A control method is required that can take into account all aerodynamic factors at every timestep in order to find an optimal trajectory. Defining the trajectory simulation as an optimisation problem allows the trajectory to be solved at every point simultaneously, producing an optimal trajectory over the entire simulation space. Optimal control theory is widely used in situations where an optimal trajectory path must be found, and has been used widely in aerospace applications. However a trajectory optimisation has not been attempted on a three stage airbreathing system, and is usually reserved for simpler systems as there can be issues with convergence and long computation times **Diehl2006**. This does not rule out using an optimisation method on a complex aerodynamic system however it does reinforce that choosing the correct optimisation procedure and defining the problem in the correct way is integral to developing an accurate solution method. This study aims

to find a method of optimisation that is applicable to a complex aerodynamic trajectory and to apply this to the SPARTAN vehicle to produce an optimal trajectory shape for maximum payload delivery to heliocentric orbit.

For an optimisation of a complex trajectory there are a variety of optimal control methods that are useful for specific problem types. These are separated into two categories: direct and indirect solution methods. Indirect methods are based on the calculus of variations or minimum principle model, and generally result in high accuracy solutions to optimisation problems **Bulirsch1993**. However indirect models suffer from the drawbacks of small radii of convergence and the fact that the equations to be solved often exhibit strong nonlinearity and discontinuities. This means that indirect methods will not be solvable unless the problem is very well defined with a minimum of nonlinearity, making indirect methods unsuitable for many complex optimisation problems such as aerospace vehicle simulations which can exhibit strong nonlinear behaviour and have a wide solution space.

Direct methods transform an optimisation problem into a nonlinear programming (NLP) problem which can be solved computationally **Stryk1992**. NLP solvers solve the optimisation problem defined as **Bazaraa2013**:

$$Minimise \quad f(x) \tag{2.1}$$

$$Subject \quad to \quad g_i(x) \leq 0 \quad for \quad i = 1,...,m \tag{2.2}$$

$$and \quad h_j(x) = 0 \quad for \quad j = 1,...,n \tag{2.3}$$

An optimisation problem that has been discretised in this form can thus be solved using any of a variety of NLP solvers. One of the most effective methods of solving twice differentiable NLP problems is sequential quadratic programming (SQP) **Boggs2000** for which there is a variety of commercial solvers available such as NPSOL, SNOPT and packages within MATLAB.

In order for these packages to be able to solve an optimisation problem it must be presented in discretised form, and as such must be transformed using approximation techniques. The task of approximating a continuous optimisation problem in discrete NLP solvable form is not simple. SQP solvers can very easily run into convergence issues when provided with an optimisation problem which has not been well defined over a logical solution space. Also, any approximation must be carried out with care that the accuracy of the solution is not compromised. There are multiple ways to approximate a continuous optimisation problem directly as an NLP problem, the most common of which are shooting and collocation methods. The differences in the behaviour of each method are related to the interaction between the SQP solver and the discretisation method by which the problem is defined, and can affect the stability and accuracy of the solution as well as the solution time of the problem. For this study of in atmosphere trajectory optimisation with complex atmospheric and

vehicle properties it was desired that a method be found with maximum stability and accuracy for a relatively large solution space, while solution time is a secondary priority.

2.8.1 The Single Shooting Method

The oldest and simplest method of approximating continuous optimisation problems as NLP problems is the direct single shooting method. Direct single shooting discretises the control function over the solution space, and solves this directly as an NLP by integrating the vehicle dynamics, or state variables, along the trajectory at each trajectory guess. Single shooting is simple to apply and has been used since the 1970s for rocket trajectory optimisation **jezewski1971**. Single shooting methods suffer from nonlinearity problems, ie. an optimisation problem solved using the single shooting method will potentially struggle to solve if the problem exhibits even small nonlinearities, due to being unable to converge to an optimal solution. This makes the single shooting method unsuitable for complex problems such as a scramjet model, as there are many nonlinear factors inherent in atmosphere and airbreathing engine modelling.

2.8.2 The Multiple Shooting Method

Direct multiple shooting is a popular solution to trajectory optimisation problems. This method solves some of the instabilities of the single shooting method by splitting the trajectory into multiple shooting arcs, and collocating these at specific time points. This creates a system of discontinuities, illustrated in Figure 2.16, which are gradually removed by the solver algorithm until the trajectory is continuous. These discontinuities allow greater flexibility for the solver than is afforded by the single shooting method. The multiple shooting problem is solved as an NLP through discretisation of the state and control variables at each time node and integration for the state variables x over each shooting arc t_k **Subchan2008**:

$$\dot{x} = v = f[x(t), u(t)] \tag{2.4}$$

With the state variables subject to the boundary conditions:

$$r[x(t_0), x(t_f)] = 0 \tag{2.5}$$

And solving for the unknown values s_i:

$$x(t_i) = s_i, \qquad i = 1, 2...N \tag{2.6}$$

The control variables at the nodes are guessed and the state variables are integrated along the trajectory, with each node segment being considered separately. A matching condition is introduced that must be met between each segment; ie. the trajectory must be continuous. **Michalik2009**

$$\mathbf{X(s)} = \begin{Bmatrix} x(t_1; s_0, v_0) - s_1 \\ x(t_2; s_1, v_1) - s_2 \\ \vdots \\ x(t_N; s_{N-1}, v_{N-1}) - s_N \\ r[x(s_0), x(s_N)] \end{Bmatrix} = \mathbf{0} \tag{2.7}$$

This is now in the form of an NLP problem which may be solved in a standard NLP solver. ie. minimise:

$$\min J(s, v) = \sum_{i=0}^{N-1} J_i(s_i, v_i) \tag{2.8}$$

subject to:

$$x[t_{i+1}, s_i, v_i] - s_{i+1} = 0 \tag{2.9}$$
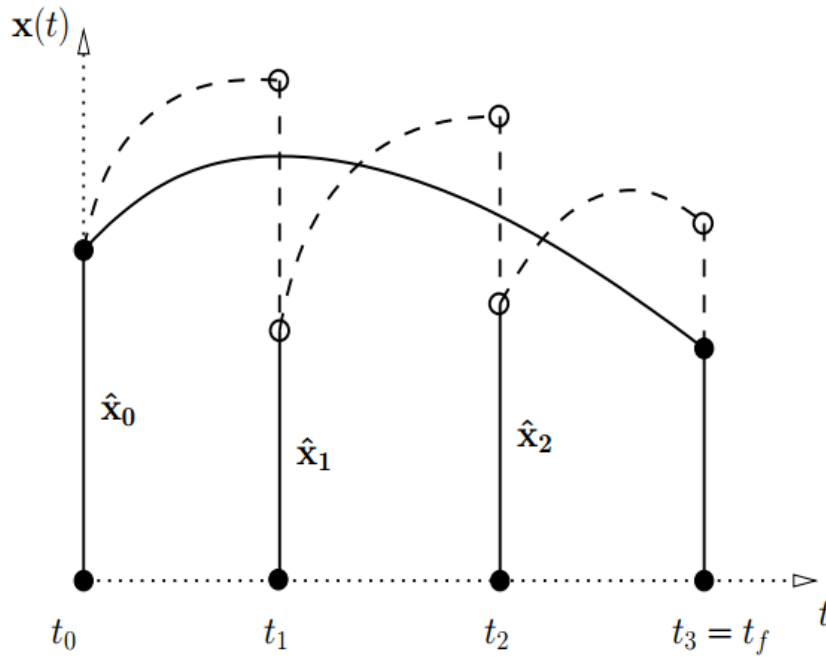
$$r[x(s_0), x(s_N)] = 0 \tag{2.10}$$

Figure 2.16: An illustration of the subdivision associated with multiple shooting **Michalik2009**. Dashed lines illustrate the initial trajectory guess and the solid line indicates the final trajectory once the joining conditions are met.

The multiple shooting method has greatly improved convergence compared to the single shooting method, removing much of the susceptibility to instabilities resulting from nonlinear effects. How-

ever, the multiple shooting approach still suffers from a relatively small radius of convergence and slow computation times. Radius of convergence is extremely important to this study as the optimal solution cannot be approximated to a great degree of accuracy, and as such multiple shooting was deemed inappropriate for this study. It was desired to find a method with a global radius of convergence to apply to the optimisation problem being considered.

2.8.3 The Pseudospectral Method

The most promising method found to address the issue of radius of convergence is the direct collocation approach, which provides global radius of convergence with the additional advantage of smaller computational time **Fasano2013**. Direct collocation methods discretise the control and state equations of the optimal control problem, and use these as constraints in an NLP problem similarly to the multiple shooting approach. However the state functions in collocation methods are approximated by polynomial functions over the solution space, inherently being continuous at each collocation node rather than the state functions being integrated over each timestep. The derivative of the state functions then become a constraint within the NLP, being equated to the polynomial approximation functions by the solver algorithm. The method used to discretise the derivative functions is very important to the accuracy of the collocation method, with trapezoidal, Hermite-Simpson and pseudospectral methods being popular choices.

The most accurate form of these as tested by Fahroo & Ross **Fahroo2000** is the pseudospectral method, which uses some elements of spectral method approximation to accurately approximate derivative terms. The pseudospectral method was first introduced in 1972 by Kreiss & Oliger **Kreiss1972** as an efficient way to compute meteorology and oceanography problems. The pseudospectral method employs the use of orthogonal polynomials such as Legendre or Chebychev polynomials to approximate the state and control functions over the solution space **Fahroo2000**. The Legendre polynomial method as used by Fahroo & Ross in 1999 **Fahroo1999** is a method of transforming a continuous optimisation problem into an NLP problem. These pseudospectral methods have the property that when evaluated at specific Legendre-Gauss-Lobatto points, the approximate state and control functions are exactly equal to the continuous function being approximated at that point. These create efficient and simple relationships for the evaluation of time-continuous optimisation problems **Fahroo2000**.

The pseudospectral method discretises the optimisation problem for application of an NLP solver. The initial form of the optimisation problem is that of a generic Bolza optimisation problem, described by a continuous Bolza cost function:

$$J(\mathbf{u}, \mathbf{x}, \tau_f) = M[\mathbf{x}(\tau_f), \tau_f] + \int_{\tau_0}^{\tau_f} L[\mathbf{x}(\tau), \mathbf{u}(\tau)] d\tau \tag{2.11}$$

Subject to a set of state dynamics, which describe the behaviour of the system over the solution

space:

$$\dot{\mathbf{x}}(\tau) = f[\mathbf{x}(\tau), \mathbf{u}(\tau)] \tag{2.12}$$

These are constrained by boundary conditions of the system at the initial and final time points:

$$\psi_0[\mathbf{x}(\tau_0), \tau_0] = \mathbf{0} \tag{2.13}$$

$$\psi_f[\mathbf{x}(\tau_f), \tau_f] = \mathbf{0} \tag{2.14}$$

These equations must be discretised in such a way that an NLP solver can produce an optimal result. The pseudospectral method discretises the cost function (Equation 2.11) as follows:

$$J[\mathbf{x}(t_k), \mathbf{u}(t_k)] = \frac{\tau_f - \tau_0}{2} \sum_{k=0}^{N} L[\mathbf{x}(t_k), \mathbf{u}(t_k)] w_k + M(\mathbf{x}t_N, \tau_f) \tag{2.15}$$

where w_k is a weighting function defined by the Legendre polynomial L_N:

$$L_N = \frac{1}{2^N N!} \frac{d^N}{dt^N} (t^2 - 1)^N \tag{2.16}$$

$$w_k = \frac{2}{N(N+1)} \frac{1}{[L_N(t_k)]^2} \tag{2.17}$$

The state equations (Equation 2.12, in this case the system dynamics) are described by:

$$\frac{(\tau_f - \tau_0)}{2} \mathbf{f}[\mathbf{x}(t_k), \mathbf{u}(t_k)] - \sum_{l=0}^{N} D_{kl} \mathbf{x}(t_l) = \mathbf{0} \tag{2.18}$$

Where D is the differentiation matrix, defined at each entry k, l by:

$$k \neq l \qquad D_{kl} = \frac{L_N(t_k)}{L_N(t_l)} \frac{1}{t_k - t_l} \tag{2.19}$$

$$k = l = 0 \qquad D_{kl} = -\frac{N(N+1)}{4} \tag{2.20}$$

$$k = l = N \qquad D_{kl} = \frac{N(N+1)}{4} \tag{2.21}$$

$$otherwise \qquad D_{kl} = 0 \tag{2.22}$$

The boundary conditions are expressed analogously to the continuous problem:

$$\psi_0[\mathbf{x}(t_0), \tau_0] = \mathbf{0} \tag{2.23}$$

$$\psi_f[\mathbf{x}(t_N), \tau_f] = \mathbf{0} \tag{2.24}$$

However the pseudospectral optimisation problem must now be subject to a set of inequality constraints defining the bounds of the problem:

$$\mathbf{g}[\mathbf{u}(t_k)] \leq \mathbf{0} \tag{2.25}$$

In the context of applying this to an trajectory optimisation problem the inequality constraints are the upper and lower bounds of the system dynamics, expressing the physical limits on the simulated trajectory.

A large advantage of the pseudospectral method is the ability to generate Hamiltonian and costate values easily, detailed by Gong et al. **Gong2010** and Fahro & Ross **Fahroo2001**. The Hamiltonian and costate values allow a solution to easily and quickly be checked for accuracy. The Hamiltonian equalling zero is a necessary (but not sufficient) condition for optimality, and the costates represent the marginal cost of violating the system constraints. In order to make a preliminary test for an optimal solution the Hamiltonian and costates must simply by observed to be close to zero.

2.8.4 Pseudospectral Examples

In order to assess the applicability of the pseudospectral method to an in atmosphere trajectory optimisation problem, the range of existing solutions utilising the pseudospectral method has been investigated. The pseudospectral method has been proven to be extremely effective for simulations in aerospace applications and has been proven in flight applications such as the zero propellant manoeuvre of the International Space Station in 2007, where the ISS was rotated 180 degrees without any propellant used following a pseudospectral method solution **Bedrossian**. The pseudospectral method

has also been utilised in the control of satellites in low Earth orbit in a study by Yan et al. **Yan2007**. The satellites were required to be stabilised utilising the Earth's magnetic field, which requires a solution to the Riccati equation to be solved in real time, a potential computation burden to the legacy systems used. The pseudospectral method was tested as a possible solution. The satellites were controlled to a desired attitude in three dimensions using both the solution to the Riccati equation and the pseudospectral method. It was shown that the pseudospectral method matched the results of existing solutions and improved on computation time over that of the Riccati solution by an order of magnitude. This indicates that the pseudospectral method is not only accurate, but computationally efficient for systems with multiple state variables.

The pseudospectral method has also been utilised for the reconfiguration of spacecraft formations in a study by Huntington & Rao **Huntington2008**. A simulated tetrahedral spacecraft formation was reconfigured using the pseudospectral orbit in a fuel optimal manner within one orbit, necessary because the initial formation was observed to degrade significantly after being simulated forwards by three weeks. A new formation was found that minimised this degradation, and the movement of the spacecraft into new positions was computed using a pseudospectral method. Figure 2.17 and Figure 2.18 show the initial and final configurations of the spacecraft respectively. This study uses five state
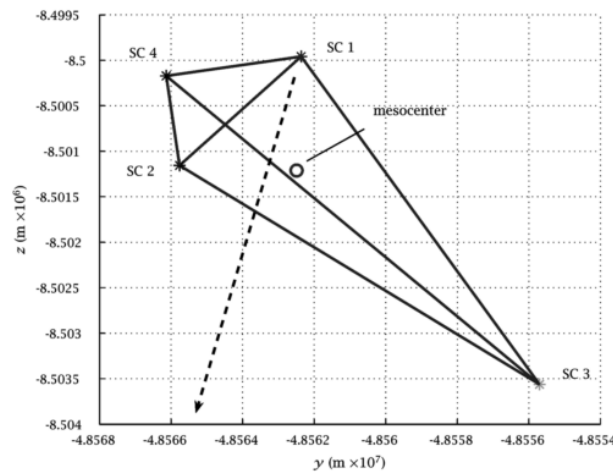

Figure 2.17: Initial spacecraft formation configuration **Huntington2008**.

variables, with complex codependency between each variable. The positive results of this study are an indication that the pseudospectral method retains accuracy for a large amount of state variables and can successfully solve when states are highly reliant on one another, as is the case for a trajectory with significant atmospheric effects.

These examples show the ability of the pseudospectral method to simulate complex simulated systems efficiently and accurately, however these examples are based on orbital dynamics and are potentially not indicative of pseudospectral method performance for more complex in-atmosphere dynamics. The pseudospectral method has been used for the guidance of re-entry vehicles including
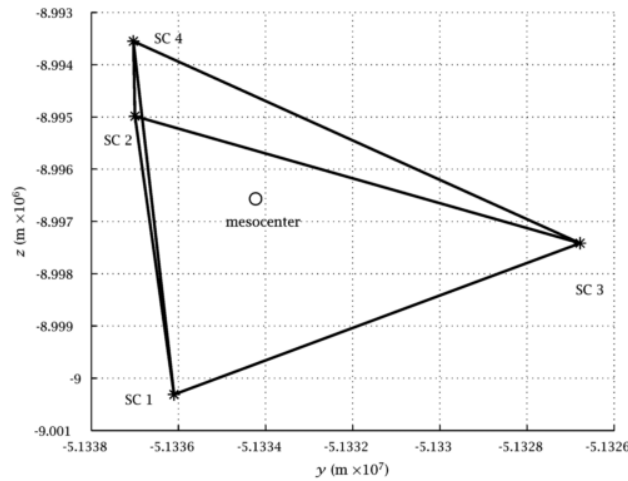
Figure 2.18: Terminal spacecraft formation configuration **Huntington2008**.

in-atmosphere dynamics, to keep a vehicle on a desired three degree of freedom path in real-time in a study by Tian & Zong **Tian2011**. The pseudospectral method was found to generate an accurate trajectory around the desired reference trajectory, satisfying all necessary constraints in real-time for six state variables with minimal error. This is a useful result as it shows that the pseudospectral method does not exhibit instabilities with nonlinear effects such as atmospheric density varying the dynamics of the system being optimised, and that the pseudospectral method can be used for systems with at least up to six state variables. Nonlinear effects are an intrinsic part of simulating a complex aerodynamic system, and this study indicates that the pseudospectral method will be able to simulate the SPARTAN vehicle and is appropriate for use in this study.

Based on the proven track record of the pseudospectral method in simulation situations, it was decided that using the pseudospectral method for the optimisation of the rocket-scramjet-rocket system was a sound and feasible decision. It has been necessary to investigate the range of solvers available that will utilise a pseudospectral method to solve an optimisation problem with the desired capabilities and usability.

2.8.5   Available Solvers

The pseudospectral method has a number of solvers available commercially, the foremost of which are DIDO, produced by Elissar Global **Ross2002**, GPOPS II **Rao2010** and PROPT, a module integrated with TOMLAB **Rutquist2010**. These solvers utilise nonlinear programming techniques to solve optimal control problems in discretised form and are all similar in their operation. These have been investigated for a variety of considerations with details available in Section **??**. The most promising of the solvers investigated is DIDO. DIDO is a pseudospectral method solver that is capable of solving complex systems with multiple variables, and outputting Hamiltonian and costate values automatically. DIDO has been used in a wide variety of disciplines, including the solution for a zero-

propellant manoeuvre of the ISS in 2006 **Bedrossian**. DIDO has been selected for use in this study after evaluation of the available options, taking into account user friendliness as well as the program track record from publications (Table **??**).

2.9 Aerodynamic Analysis

- preliminary design requires fast and easy aerodynamics

Simulating the trajectory of access to space vehicles requires the aerodynamics of the launch vehicle to be characterised accurately. This entails the creation of large aerodynamic coefficient databases, which cover the operable region of the vehicle, and include the effect of control surface deflections. The liability of the vehicle design to change during the preliminary design phases renders highly accurate CFD or experimental studies expensive and inefficient CITATION. Instead, solutions are found which are able to approximate the aerodynamic characteristics to an appropriate accuracy, while providing fast set-up speeds as well as computation times.

2.9.1 HYPAERO

Hypaero is an aerodynamic calculation tool developed for the preliminary design of hypersonic vehicles. HYPAERO uses strip theory, dividing the surface of the vehicle into panels to calculate aerodynamic properties along the aircraft as illustrated in Figure 2.19. In strip theory two dimensional sections are created running the length of the vehicle, defining streamlines along the vehicle faces. Pressure, Mach number and skin friction are calculated along these streamlines to compute the aerodynamic coefficients of the vehicle. The Aerodynamic analysis of the SPARTAN has been performed using HYPAERO by Jazra et al. **Jazra2013**. The aerodynamic coefficients of the SPARTAN vehicle have been provided for this study by Dawid Preller.

2.9.2 CART3D

CART3D is an inviscid CFD package, designed for use during preliminary vehicle design and analysis CITATION. CART3D requires only a surface triangulation of the vehicle being analysed. CART3D features adjoint mesh adaption, and uses cartesian 'cut-cells' which intersect the surface, allowing complex geometries to be analysed. The mesh automatically refines as the simulation progresses, reducing error. The absence of a requirement for a user generated mesh allows CART3D to be easily applied to complex launch vehicle designs, as well as allowing for simple modification of control surface deflections and flight conditions. CART3D has been used extensively for aerodynamic simulations in preliminary design, including analysis of the Skylon spaceplane**Mehta2016**, HIFiRE-5**Kimmel2010**, and in low sonic boom shape optimisations**Aftosmis2011**. Mehta et al. used CART3D to analyse
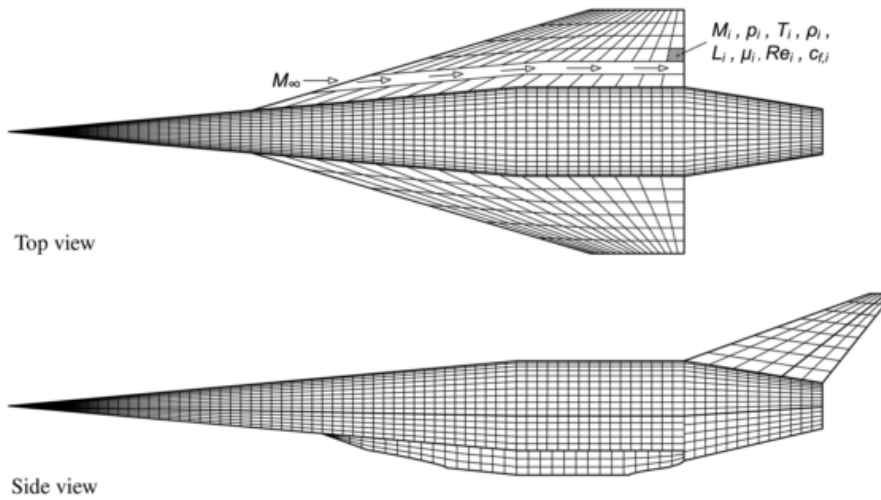
27

Figure 2.19: HYPAERO analysis surface grid **Jazra2013**.

the Skylon spaceplane, in a study which investigated the aerodynamics of the vehicle as well as the plumes produced by the Reaction Engines LTD SABRE engines**Mehta2016**. The Skylon was analysed at a range of mach numbers from 2.625 to 16.969, at altitudes from 15.326km to 75.771km. These results indicate the applicability of CART3D over a wide range of Mach numbers, which is of particular use to this study. During a study by Aftosmis & Nemec where CART3D was applied to low sonic boom shape optimisation, CART3D was shown to have good agreement with experimental results in tests at Mach 1.6.

The wide Mach number range of CART3D, along with its ease of use and demonstrated accuracy, makes CART3D a useful tool for this study.

2.9.3 Missile DATCOM

Missile DATCOM is a widely used, semi-empirical, aerodynamic prediction tool for missile configurations. Missile DATCOM is capable of calculating the aerodynamic forces, stability derivatives and moments over a range of angle of attack and Mach number values, allowing an aerodynamic database to be generated simply and rapidly. Missile DATCOM has been shown to produce close agreement with experimental wind tunnel data for normal force and pitching moment coefficients, and reasonable agreement for axial force coefficients **Sooy2005**.

2.10 Summary

This chapter has reviewed literature relevant to this thesis. Add more details.
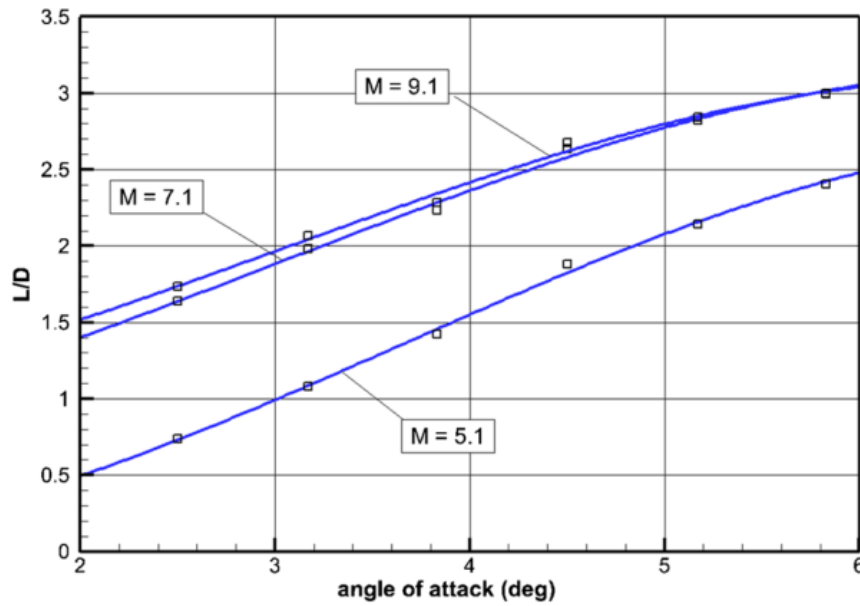
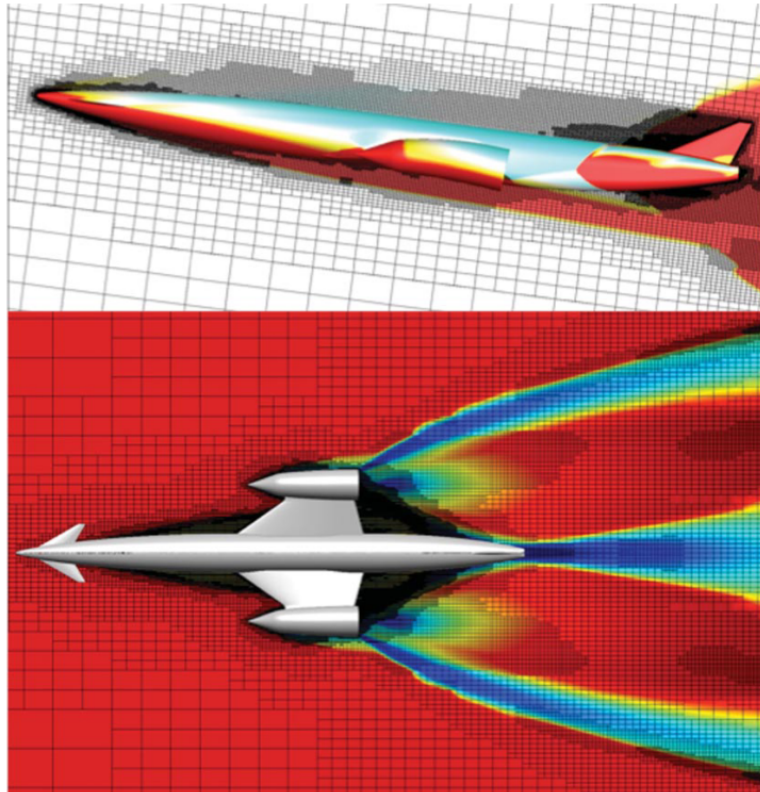Figure 2.20: SPARTAN aerodynamics, developed using HYPAERO **Preller2017**.

Figure 2.21: The Skylon spaceplane, simulated using CART3D at Mach 12.189, $\alpha = 7.512°$**Mehta2016**. Cell distribution produced by mesh adaption is shown.

LAUNCH VEHICLE BASELINE DESIGN

This chapter presents the baseline three stage small satellite launch system utilised in this thesis. The design for the first stage rocket-powered vehicle, second stage scramjet-powered vehicle (the SPARTAN), and third stage rocket-powered vehicle are presented. This baseline design is used for the initial trajectory analysis and optimisation in this study. The launch system has been designed based on the SPARTAN vehicle developed by Preller & Smart.

This chapter also describes the aerodynamic models of the vehicles used in this study, including the engine models.

3.1 First Stage Rocket

The first stage rocket-powered vehicle is based on the first stage of the SpaceX Falcon-1e. The Falcon-1e has been chosen due to its appropriate scale, and the proven flightworthiness of the Falcon-1.
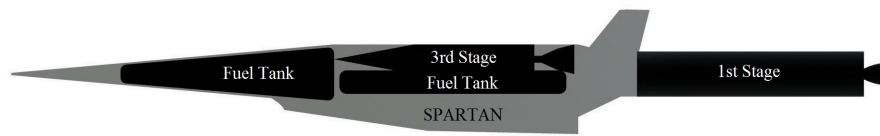

22.94m	9.5m
SPARTAN	First Stage Rocket
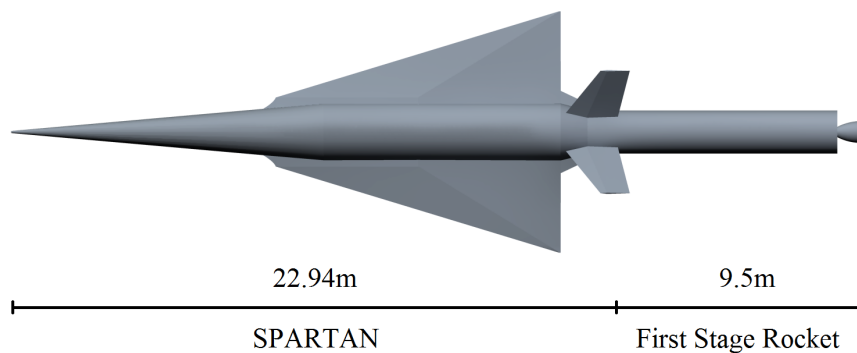
Figure 3.1

Figure 3.2

detailed design First Stage CART3D - details of CAD, pointwise mesh, and CART3D gridding settings

3.2 Second Stage Scramjet

3.2.1 Baseline Vehicle

The SPARTAN vehicle in this study has been designed based on the work by Preller & Smart CITATION.

The baseline SPARTAN has been designed to hold a 9 m long third stage. Two cylindrical tanks underneath the third stage and a conical tank situated in the nose have a total volume of 22.0m3 and hold a total of 1562kg of LH2 fuel. This assumes an LH2 density of 71kg/m3, slightly denser than LH2 at phase transition point at 1 atm.

fuel tanks are sized to include a kestrel third stage

total tank volume = 22m^3

gives a fuel mass of 1562kg

Dawid has a fuel tank volume of 14.01m^3, mass of 132.8kg

using $22^2/3$ / $14.01^2/3$ to approximate surface area ratio

mass of new tank is 1.351*132.8 = 179.41kg

CG - determined using CREO

3.2.2 Aerodynamics

method of calculating aerodynamics for trim at required lift

conical shock calculation

CART3D lift/drag

Images of CART3D results for a range of Mach numbers

3.2.3 Propulsion Modelling

The SPARTAN is powered by four underslung scramjet engines. These engines are Rectangular To Elliptical Shape Transition (REST) engines, configured to allow for a conical forebody (C-REST).
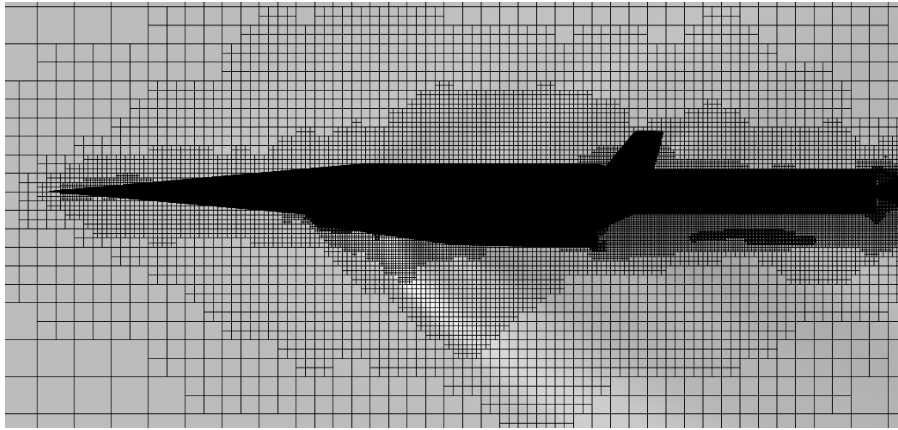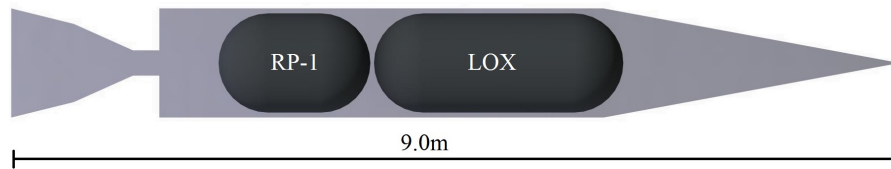
Figure 3.3

Figure 3.4

The engine model used is a CRESTM10, analysed using quasi-1D simulation. The specific impulse and equivalence ratio data sets are shown in Figure XXX. The specific impulse and equivalence ratio during flight are determined by interpolating these data sets. As the equivalence ratio is equal to 1 in the majority of the Mach number and temperature regime, only the regions in which it is less than 1 are used for the interpolation. The equivalence ratio interpolation is linear, as the number of data points available for interpolation is low.

3.3 Third Stage Rocket

The third stage vehicle has been designed to accommodate a SpaceX Kestrel engine. The Kestrel has been chosen for its cost effectiveness and proven capabilities.

The third stage rocket is released at the end of the scramjet accelerator burn, and lifts the payload out of the atmosphere and into the desired orbit. The third stage weighs a total of 3300kg. The third stage has a structural mass fraction of 0.09, similar to the Falcon 1 second stage **Vehicle2008**. This gives a total structural mass of 285.7kg.

The kestrel engine has been modified to have 50% increased propellant mass flow rate, giving a mass flow rate of 14.8kg/s. The nozzle of the Kestrel engine has been kept at XXXm diameter. This increase in mass flow results in a 2% loss of efficiency from the nozzle (CITATION). The modified specific impulse of the engine is 310.7s.

33

Area = 0.866

Lnose = 3m, Centrebody = 4.5m, Engine = 1.5m. Note, some room has been left for the kestrel to go into the body slightly (about 0.5m)

CG - determined using creo, assumed that structure is homogeneous for simplicity

3.3.1 Fuel Tank Sizing

The fuel tanks have been sized assuming 100kg of payload-to-orbit. Note that the method of calculating final payload-to-orbit relies on using left over 'fuel mass' as effective payload mass. Realistically this would cause the fuel tanks to be resized slightly. For the purposes of this study the fuel tanks have been assumed to be of constant size for simplicity. Currently this is a reasonable assumption as the internals of the rocket are very simplified. The structural mass is held constant at 9%.

Propellant mass: 2736.7 kg.

Propellant ratio is 2.56 LOX : 1 RP1

mass LOX = 1968.0 kg. ρ_{LOX} = 1141kg/m3. volume LOX = 1.7248m3

mass RP1 = 768.7 kg. ρ_{RP1} = 813kg/m3. http://nvlpubs.nist.gov/nistpubs/Legacy/IR/nistir6646.pdf

volume rp1 = 0.9455m3

3.3.2 Aerodynamics

Third Stage missile DATCOM details

3.3.3 Thrust Vectoring

The third stage rocket is trimmed during the in-atmosphere portion of its ascent trajectory via thrust vectoring. The centre of pressure is calculated using missile DATCOM. The thrust vector is set so that the moment generated by the engine matches the lift force acting at the centre of pressure. The maximum thrust vector limit has been set to $8°$. As no data on the maximum thrust vectoring capabilities of the kestrel engine was able to be found, this was set to the maximum gimbal range of the Aestus pressure-fed engine and OMS, similar pressure fed engines.

3.3.4 Heat Shield Sizing

The third stage is protected while in-atmosphere by a heat shield, weighting 130.9kg. This heat shield is constructed from a phenolic cork cylinder, a reinforced carbon-carbon nose cone, and a tungsten nose tip.

The tungsten nose is 50mm diameter, at the end of a 50mm Cylinder. The density of tungsten is $\rho_{Tungsten} = 19.25$ g/cm^3, giving a total mass for the nose of m = 12.6kg.

Carbon-Carbon shell $\rho_{CC} = 1800$ kg/m^3 Thickness of 10mm L = 3m R = 0.525 Area = 5.0232m2 (from Creo)

Anose = 6.22e-2 m2

m = (Area - Anose) t ρ = 89.3kg

Cork Cylinder t = 5mm $\rho_{Cork} = 320$ kg/m^3

Area = 14.844m2

m = 23.7kg

$m_H S$ = 125.6kg

CHAPTER 4

LODESTAR

Ingo said maybe have an example in here illustrating the optimisation. maybe something from a textbook.

The program LODESTAR (Launch Optimisation and Data Evaluation for Scramjet Trajectory Analysis Research) has been developed to aid with the simulation and trajectory optimisation of space launch systems. LODESTAR is a MATLAB based trajectory optimiser which utilises DIDO, a proprietary pseudospectral method optimisation package as well as MATLAB's inbuilt SQP solver. LODESTAR optimises a trajectory towards a user-defined objective function, such as constant dynamic pressure or maximum payload-to-orbit. LODESTAR accurately models both rocket-powered and scramjet-powered vehicles in 5 degrees of freedom. LODESTAR contains multiple modules configured for the SPARTAN launch system, which are able to optimise trajectories for;

1. The ascent of the first stage rocket.

2. The ascent of the second stage scramjet-powered accelerator.

3. The flyback of the second stage scramjet-powered accelerator.

4. The ascent of the third stage rocket.

4.0.1 Optimal Control

The pseudospectral method and direct single shooting techniques used by LODESTAR are described in detail in sections X-X. Practically, the implementation of these techniques involves the specification of the set of constraints and objectives which govern the optimisation problem. These constraints inform the optimiser of the limits of the optimisation, and perform the functions of bounding the logical search space (eg. constraining altitude to be greater than ground level) as well as constraining

the vehicle within its performance limits (eg. limiting the angle of attack). These constraints also come in the form of initial or terminal constraints, which define the initial conditions of the trajectory as well as any conditions which the trajectory must meet at termination.

The pseudospectral method requires the specification of a set of 'primal variables'. These primal variables describe the physical dynamics of the system. In the pseudospectral method, the dynamics of the system are used as constraints on the optimal control problem;

$$\dot{\mathbf{x}}(\tau) = f[\mathbf{x}(\tau), \mathbf{u}(\tau)]. \tag{4.1}$$

Implementing the dynamics as constraints allows the optimiser to explore each primal variable independently, greatly increasing the robustness of the optimal control problem. However, the constraints may be violated by the optimiser in the process of searching for an optimal solution. A violation of the physical dynamics constraints means that the dynamics of the system may not hold throughout the solution process, causing potential complications for the computational model of the vehicle. Much of the design of the vehicle simulation in this study is driven by the need for smooth, continuous interpolation schemes, and viable extrapolation regions ie. even if the solution is well within the range of all input data sets, the solver must be able to explore all regions within the set bounds.

4.0.2 Dynamic Model

The drag and lift produced by each stage of the vehicle are calculated using the standard definition of the aerodynamic coefficients:

$$F_d = \frac{1}{2}\rho c_d v^2 A, \tag{4.2}$$

$$F_L = \frac{1}{2}\rho c_L v^2 A. \tag{4.3}$$

The dynamics of all stages are calculated using an geodetic rotational reference frame, written in terms of the radius from centre of Earth r, longitude ξ, latitude ϕ, flight path angle γ, velocity v and heading angle ζ. The equations of motion are **Josselyn2002a**:

$$\dot{r} = v \sin \gamma \tag{4.4}$$

$$\dot{\xi} = \frac{v \cos \gamma \cos \zeta}{r \cos \phi} \tag{4.5}$$

$$\dot{\phi} = \frac{v \cos \gamma \sin \zeta}{r} \tag{4.6}$$
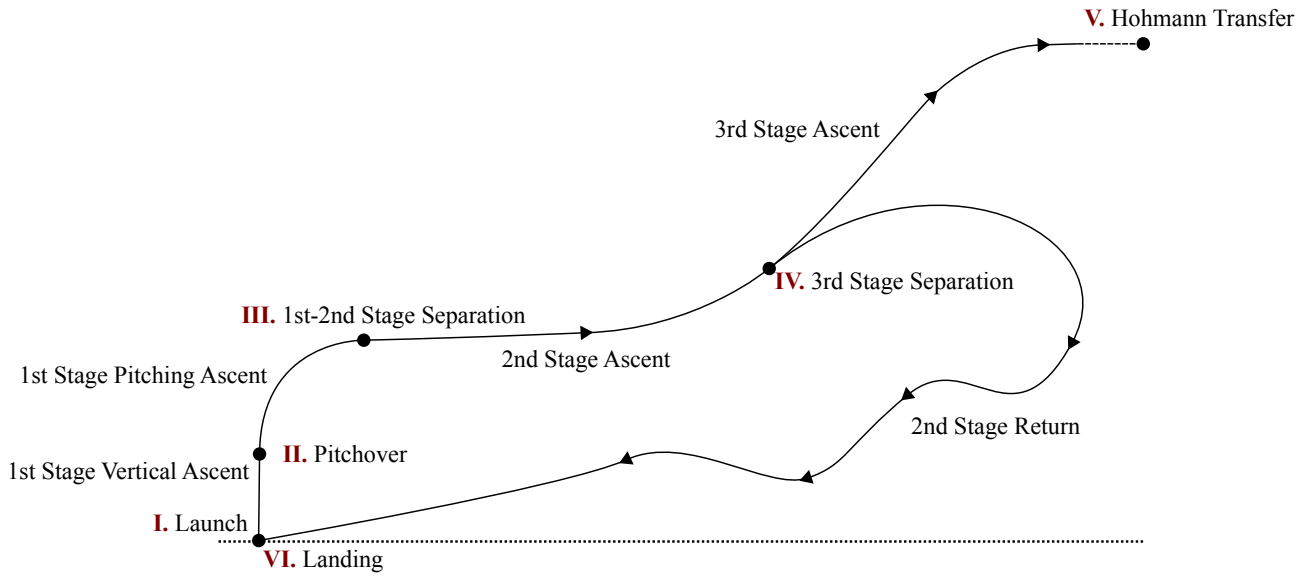
Figure 4.1

$$\dot{\gamma} = \frac{T \sin \alpha \cos \eta}{mv} + (\frac{v}{r} - \frac{\mu_E}{r^2 v}) \cos \gamma + \frac{L}{mv} + \cos \phi [2\omega_E \cos \zeta + \frac{\omega_E^2 r}{v}(\cos \phi \cos \gamma + \sin \phi \sin \gamma \sin \zeta)]$$
(4.7)

$$\dot{v} = \frac{T \cos \alpha}{m} - \frac{\mu_E}{r^2} \sin \gamma - \frac{D}{m} + \omega_E^2 r \cos \phi (\cos \phi \sin \gamma - \sin \phi \cos \gamma \sin \zeta)$$
(4.8)

$$\dot{\zeta} = \frac{T \sin \alpha \sin \eta}{mv} - \frac{v}{r} \tan \phi \cos \gamma \cos \zeta + 2\omega_E \cos \phi \tan \gamma \sin \zeta - \frac{\omega_E^2 r}{v \cos \gamma} \sin \phi \cos \phi \cos \zeta - 2\omega_E \sin \phi$$
(4.9)

Flow chart of modules details of simulation (5DOF geodetic rotational) details of limits

verification methods -hamiltonian/costates -complementary conditions -forward sim (for sanity checking, will need to detail deficiencies in this) -forward integration -logic check (ie solver is still a heuristic process, run multiple times with varying guess. Is solution logical?)

-Geodetic rotational coordinates -put coordinate system here -Pontani has a typo is his paper remember -add in portion of lift going towards changing heading angle due to roll. This is just simple centripetal force. $F = mr\omega^2$ $v = \omega r$

- outline the pseudospectral method, as implemented in GPOPS? ie with stage definitions

4.0.3   Trajectory Connection Points

image here detailing the trajectory and separation points, including what the constraints of each trajectory are. Maybe number these separation points, and refer to these numbers in th constraint table for each trajectory stage.

Flow chart here of how the main LODESTAR modules connect with reference to the trajectory diagram as well

4.0.4 First Stage Trajectory

-detail the vehicle dynamics with a free body diagram

LODESTAR is able to optimise the first stage of a launch vehicle, for an angle of attack controlled trajectory, from launch to a pre-defined end point. LODESTAR is able to optimise for either a maximum velocity or minimum mass optimisation objective.

A maximum velocity case is desired when a specific first stage vehicle design is being investigated.

A minimum mass objective is applicable when the first stage trajectory has a pre-defined end goal. This is the case with the SPARTAN vehicle where the SPARTAN scramjet accelerator is to be released at its minimum operating conditions at close to horizontal flight. A variable mass for the first stage launch vehicle is desired as the mass has large effects on the dynamics of th vehicle, effecting the trajectory angle change rate, as well as the acceleration and time of flight of the vehicle. It is useful in the preliminary design stages to be able to optimise the mass of the first stage vehicle, allowing a less trial-and-error approach. Note that in the minimum mass case, the launch altitude is slightly variable, as LODESTAR starts optimisation from the pitchover time, and the pre-pitchover trajectory is calculated to match the pitchover mass.

Input	Contains
Aerodynamic Database	

The first stage is launched from an area in northern Queensland.

Initial Constraints	
Terminal Constraints	
Path Constraints	
Target Cost	

Control Variables

Primal Variables

4.0.5 Second Stage Trajectory

-detail the vehicle dynamics with a free body diagram

LODESTAR is able to optimise the trajectory of airbreathing accelerators in the supersonic or hypersonic regime. LODESTAR is able to optimise for a range of optimisation metrics, including a maximum payload-to-orbit and constant dynamic pressure. The trajectory of the SPARTAN scramjet-powered accelerator has been simulated in LODESTAR.

Initial Constraints	Velocity
	Fuel Mass
	Latitude
	Longitude
Terminal Constraints	Fuel mass
	Heading Angle
Path Constraints	Dynamic Pressure
Target Cost	Maximum Payload-to-Orbit

Control Variables

Primal Variables

primal variable limits:

4.0.6   Second Stage Return Trajectory

After releasing the third stage rocket, the scramjet-powered second stage must return back to an area close to the initial launch site. During the flyback, the SPARTAN cannot exceed its dynamic pressure limit of 50kPa. The SPARTAN must land on the ground with minimum velocity, within close proximity to the launch area. It is assumed that a landing strip is available at the spot where the SPARTAN lands. The SPARTAN is required to land within a set radius of the launch site. This constraint is;

$$(\phi_{end} - \phi_{launch})^2 + (\xi_{end} - \xi_{launch})^2 - r^2 \leq 0 \tag{4.10}$$

Summary Table

Initial Constraints	Altitude
	Velocity
	Flight Path Angle
	Heading Angle
	Latitude
	Longitude
Terminal Constraints	Distance From Launch Site
Path Constraints	Dynamic Pressure
Target Cost	Minimum End Velocity

Control Variables

4.0.7 Third Stage Trajectory

-detail the vehicle dynamics with a free body diagram

Input	Contains
Aerodynamic Database	Mach Number, AoA, CA, CN, CD, CL, cP

Output	Contains

The third stage is required to deliver the payload into heliosynchronous orbit. The heliosynchronous orbit chosen is 566.89km.

Initial Constraints	
Terminal Constraints	
Path Constraints	Angle of Attack
Target Cost	

-Detail the hohmann transfer

Control Variables

4.0.8 Combined Second Stage Ascent & Return Trajectory

4.0.9 Validation

Optimality Conditions

Hamiltonian = 0 because dH/dt = 0 (Hamiltonian does not depend explicitly on time) except at end due to final time being free. Costates Complementary conditions

Forward Simulations

-both the control check and derivative check

CHAPTER 5

ASCENT TRAJECTORY

- keep this DIDO and hypaero and direct shooting

-explain why I moved to other GPOPS and CART3D at the end of the chapter

5.1   Third Stage trajectory

-Details on methodology -outline the limits that I put on it (ie cant go below starting altitude) -I should maybe run a case without these limits to show the difference -outline necessity for differing guess (will need to cite this as a regularly used process)

5.2   SPARTAN trajectory

-constant q -45kPa,50kPa and 55kPa limited trajectories -high drag trajectory

-it might be interesting to compare different third stage rocket engines
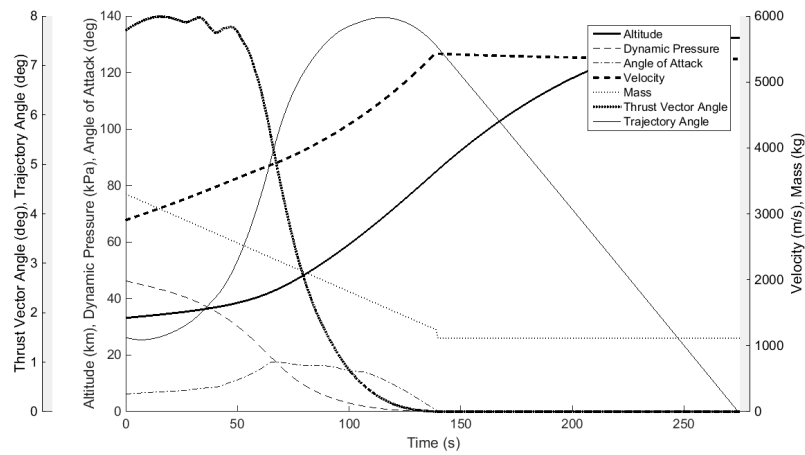
Figure 5.1
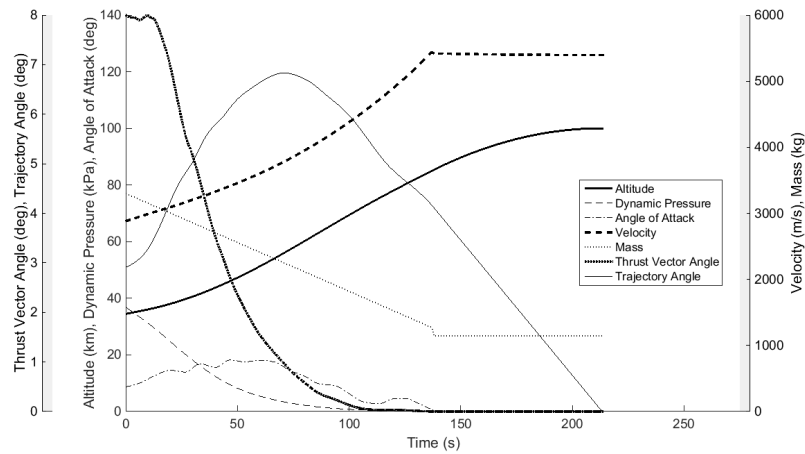
Figure 5.2
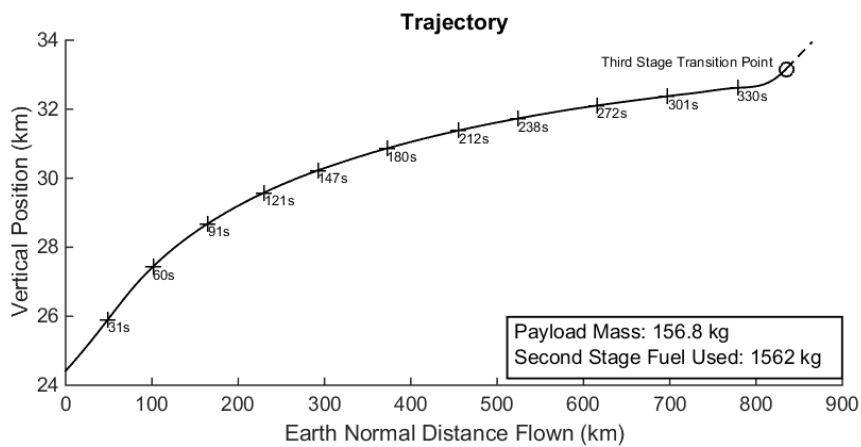
Figure 5.3
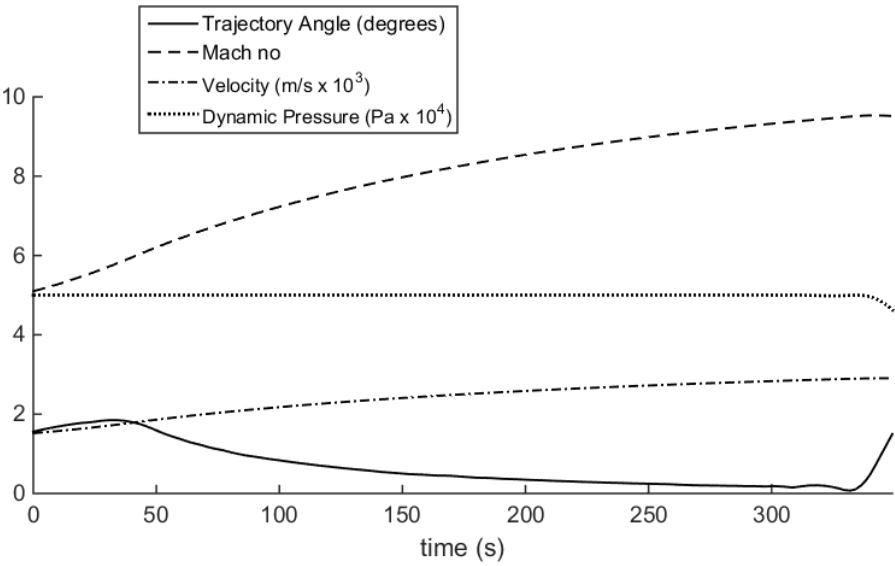
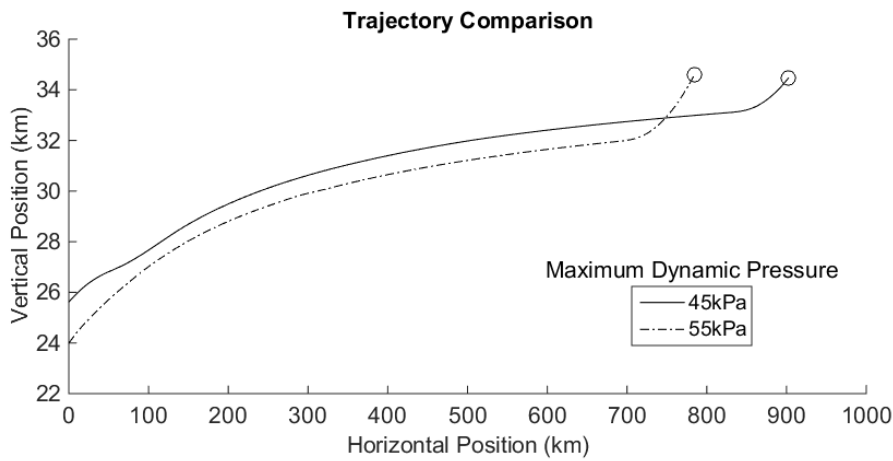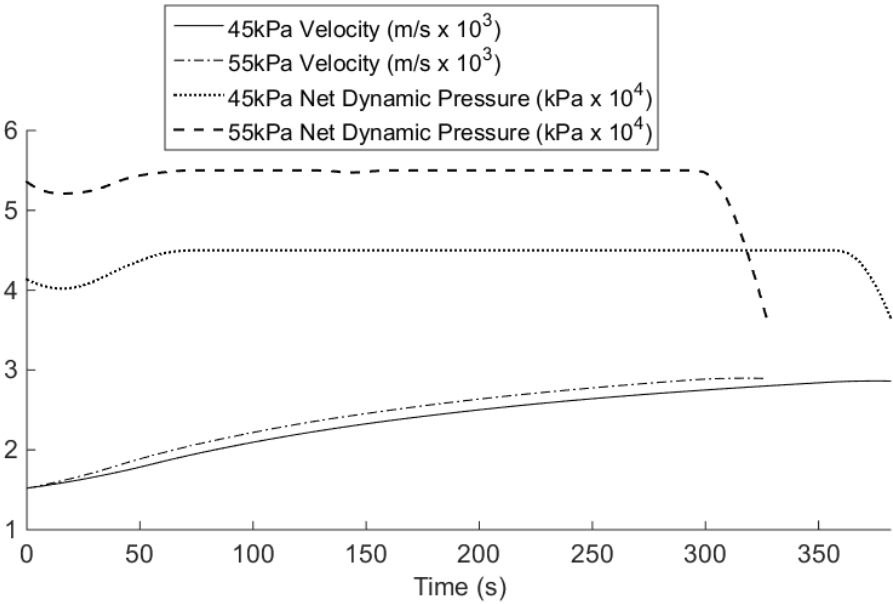Figure 5.4
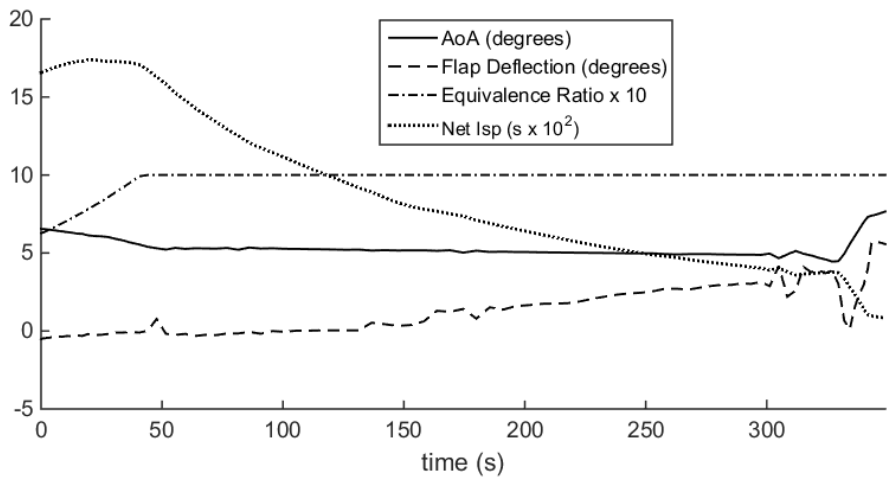
Figure 5.5
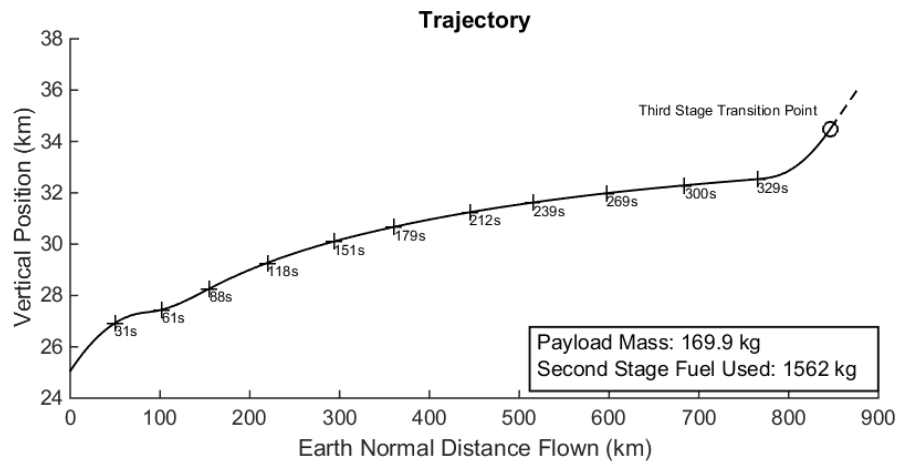
Figure 5.6
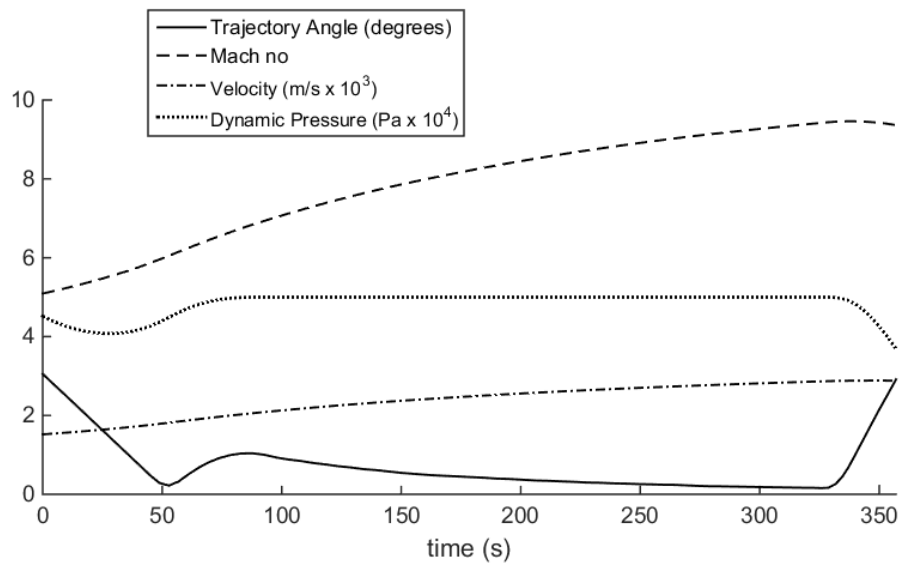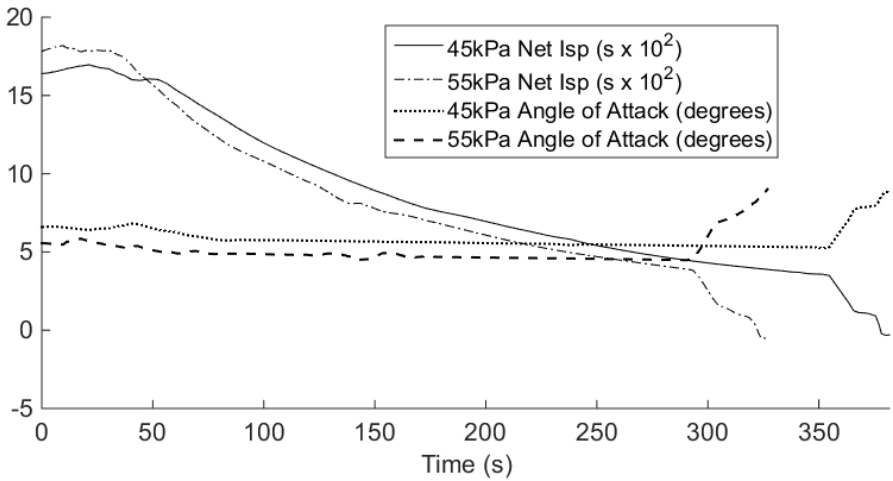

Figure 5.7
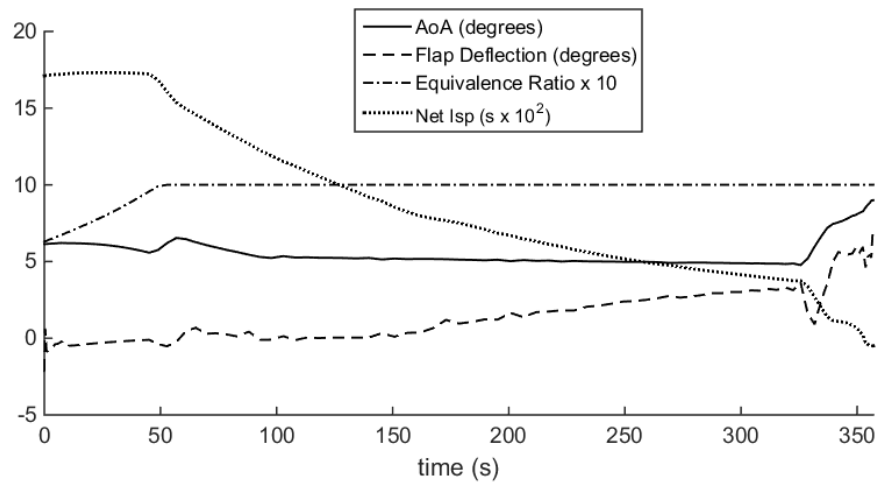
Figure 5.8

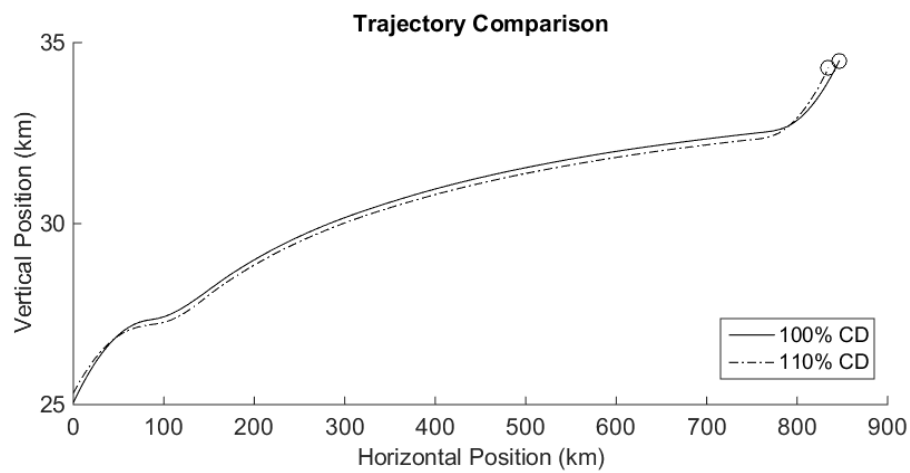
Figure 5.9

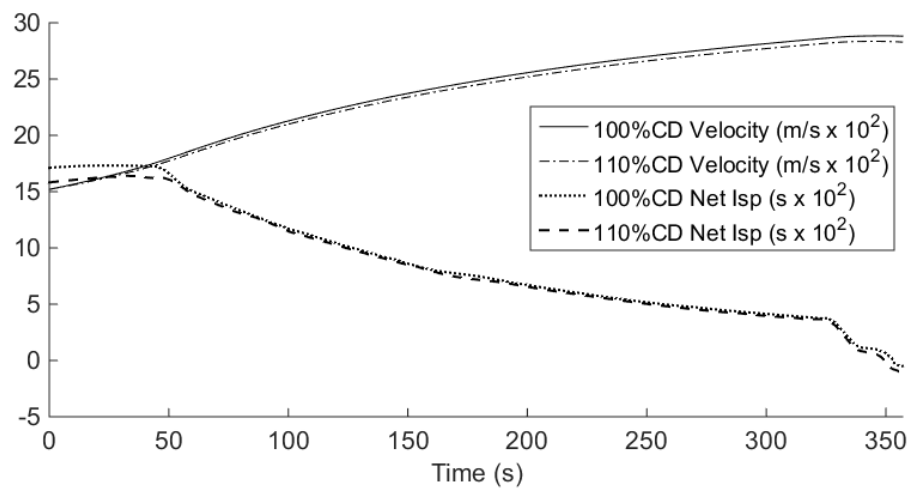Figure 5.10

Figure 5.11

Figure 5.12

Figure 5.13

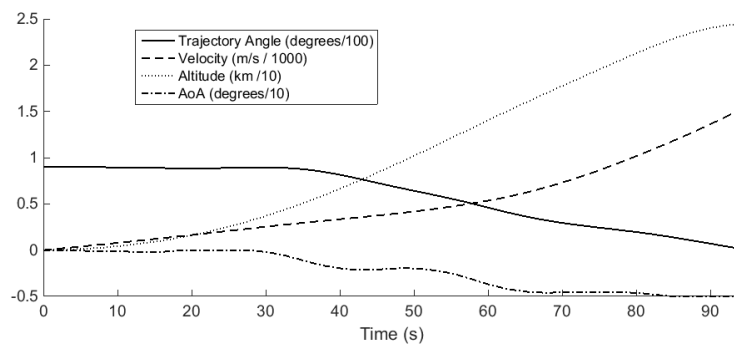Figure 5.14

5.2.1 Constant Dynamic Pressure

Optimality Validation

5.2.2 Optimal Payload

5.2.3 Maximum Dynamic Pressure Variation

5.2.4 Additional Drag Design Study

5.3 First Stage Trajectory

multiple release points -fixed mass, optimal velocity -fixed velocity, optimal mass

5.4 Flyback trajectories

-first stage to subsonic flight? -second stage Abort analysis?

CHAPTER 6

TRAJECTORIES INVOLVING FLYBACK

6.1 Flyback trajectories

-first stage to subsonic flight? -second stage Abort analysis?

CHAPTER 7

DESIGN STUDY

change the third stage design and see what different payloads come out of it.

CHAPTER 8

CONCLUSIONS

The overall aim of this thesis was to

> *the goal of my thesis was to write this document*.

Paragraph summarising what you did to achieve the above. Relate back to your text in your introduction as well.

The main conclusions that may be drawn from the work conducted in this thesis are:

Conclusion 1: Paragraph explaining conclusion.

Conclusion 2: Paragraph explaining conclusion.

Conclusion 2: Paragraph explaining conclusion.

8.1   Recommendations for future work

Things you didn't have time to do but wanted to.

Future work 1: This should be done.

Future work 2: This as well.

Future work 3: Something I forgot to do.

APPENDIX A

DETAILS OF TEST CONDITIONS